

MATHICSE Technical Report

Nr. 1.2012
January 2012



A posteriori error estimate in quantities of interest for the finite element heterogeneous multiscale method

Assyr Abdulle, Achim Nonnenmacher

A POSTERIORI ERROR ESTIMATE IN QUANTITIES OF INTEREST FOR THE FINITE ELEMENT HETEROGENEOUS MULTISCALE METHOD

A. ABDULLE AND A. NONNENMACHER

Abstract. We present an *a posteriori* error analysis in quantities of interest for elliptic homogenization problems discretized by the finite element heterogeneous multiscale method. The multiscale method is based on a macro-to-micro formulation, where the macroscopic physical problem is discretized in a macroscopic finite element space and the missing macroscopic data is recovered on-the-fly using the solutions of corresponding microscopic problems. We propose a new framework that allows us to follow the concept of the (single-scale) dual-weighted residual method at the macroscopic level in order to derive *a posteriori* error estimates in quantities of interests for the multiscale problem. Our framework allows to derive local error indicators in the macroscopic domain that can be used for adaptive, goal-oriented mesh refinement. These error indicators are defined such that they only depend on available macroscopic and microscopic solutions. We further provide a detailed analysis of the data approximation error, including the quadrature errors. Numerical experiments confirm the efficiency of the adaptive method and the effectivity of our error estimates in the quantities of interest.

Key words. multiscale problems, elliptic problems adaptive FEM, quantity of interest, homogenization, heterogeneous multiscale method

AMS subject classifications. 65N30, 65M60, 74Q05, 74Q20

1. Introduction. Multiscale models are nowadays found in many areas of science and engineering. They are for example crucial for the adequate simulation of groundwater pollution through infiltration of a fluid in a porous medium, or for finding the effective properties of composite materials important for various engineering applications. Multiscale models are also increasingly used in medicine for example to find the mechanical properties of heterogeneous tissues such as bones that are important to understand failure or diseases.

In principle, a numerical approximation of such problems could be obtained by using a standard numerical method such as the finite element method (FEM). However, the numerical approximation only converges, if we can resolve the finest length scale (the microscopic length scale) of the multiscale problem by the finite element discretization mesh size. If this microscopic length scale is small in comparison to the macroscopic length scale of the multiscale problem, then the discrete approximation leads to a problem with very large degrees of freedom (DOF) and the computational complexity becomes often overwhelming. Simply ignoring the fine-scale microscopic structure leads to numerical results that do not appropriately reflect the true physical problem, as the microscopic structure significantly influences the macroscopic behavior.

In recent years there has therefore been a considerable effort put into the design of multiscale methods for elliptic PDEs that take into account the scale separation between macroscopic and microscopic models. Babuška and Osborn [17, 16] developed the pioneering work for multiscale FEM for elliptic problems using multiscale basis functions. We further mention the multiscale finite element method (MsFEM) developed by Hou et al. [41] (see also the book by Efendiev and Hou [35]), the two-scale FEM proposed by Matache, Babuška and Schwab [48], the variational multiscale method by Hughes et al. [43], and the sparse FEM introduced by Hoang and Schwab [40]. In this work we use the framework of the heterogeneous multiscale method

(HMM) proposed by E and Engquist [31, 32, 33]. In the HMM framework, one assumes that a macroscopic description of the multiscale problem exists, even though it may not be known explicitly. This macroscopic problem is solved on a coarse mesh using a macroscopic FEM. As the data of the effective problem (e.g., the conductivity tensor) is not known it is reconstructed on-the-fly by solving microscopic problems on sampling domains located within the respective macroscopic elements. The HMM is related to numerical homogenization methods, where the fine scales are averaged out in order to obtain effective (homogenized) equations. For elliptic problems, a semi-discrete *a priori* analysis for the FE-HMM was given in [13, 34] and a fully discrete analysis was obtained in [1, 3, 9]. Furthermore, discontinuous Galerkin FE-HMM was developed in [4, 7] and problems in elasticity were studied in [2]. See also [5] for a thorough overview.

A crucial issue when using a numerical scheme is that of estimating the error or the reliability of an actual computed solution. The goal of *a posteriori* error estimates is not only to offer a criterion that indicates whether a certain prescribed accuracy is met, but also to give local error indicators, which can be used to drive an adaptive mesh refinement that equi-distributes the approximation error among the elements and therefore minimizes the total computational effort. Since the pioneering work of Babuška and Rheinboldt [18], numerous results on this research topic have been obtained and a vast literature on *a posteriori* error analysis for (single scale) elliptic PDEs is nowadays available (see for example [14], Verfürth [62] and Babuška and Strouboulis [19] and the references therein). For multiscale problems however, the literature is much more scarce. Among the few existing adaptive multiscale methods, we mention the approach based on the variational multiscale method by Hughes et al. [42, 43], which decomposes the solution into a coarse-scale and a fine-scale part. The solution of the fine-scale equation is formulated in dependence of the residual of the macro solution. *A posteriori* error estimates in the energy norm (only upper bounds) were derived by Larson and Målqvist in [47] and duality-based error estimates in [46]. First *a posteriori* error estimates for the FE-HMM have been obtained by Ohlberger [56]. These estimates are based on a reformulation of the FE-HMM in a two-scale framework [51]. We also mention the recent *a posteriori* error estimates, still in a two-scale framework, for monotone operators [39]. First *a posteriori* error estimates for the FE-HMM in the physical energy-norm have been obtained in [10, 12]. The improvement in computational efficiency that is obtained by introducing adaptivity is significant as solutions of the problems on the microscopic scale (the main computational cost of the FE-HMM) may be re-used in an adaptive mesh refinement strategy [12].

In practical applications, scientists and engineers are however often more interested in errors in a certain quantity of interest that is needed for an engineering design decision than in errors in the energy norm. Such quantities of interests can for example be an average heat flux through a certain boundary, local averages of the solution in a particular region of interest, etc. In turn, goal-oriented error estimates in quantities of interest have been developed. In the late 1990s. The general approach is as follows. Assuming that the quantity of interest can be represented by a linear bounded functional $J : V \rightarrow \mathbb{R}$ of the solution, the task is then to estimate $J(u - u^H)$, where u is the exact solution of the problem and u^H is its FE approximation. Expressing $J(u - u^H)$ in terms of an exact representation of local error estimators and higher order terms (using so-called primal and dual problems), one

can implement the following cycle

Solve \rightarrow Estimate \rightarrow Mark \rightarrow Refine

using suitable local error estimators, until the error $|J(u - u^H)|$ in the estimate step is smaller than a predefined tolerance. Among the different strategies we mention the work of Prudhomme and Oden [57, 54], Bangerth and Rannacher [20] and Becker and Rannacher [22]. The latter developed the so-called dual-weighted residual (DWR) method. The reliability of the DWR method was further investigated by Nochetto et al. [52] and Ainsworth and Rankin [15]. A general overview of adjoint methods in *a posteriori* analysis can be found in Giles and Suli [37] (see also the review by Grätsch et al. [38] and the references therein). Finally, a goal-oriented method aiming at adaptively controlling various models of a multiscale problem has been developed by Oden and co-worker [55].

The modeling and analysis of *a posteriori* error estimates in quantities of interest have not yet been developed for numerical homogenization methods to the best of the authors' knowledge. In this work we propose goal-oriented *a posteriori* error estimates for the FE-HMM. We follow the framework of the dual-weighted residual that is extended to multiscale problems. Based on appropriate modeling of multiscale fluxes, we provide a representation of the error in terms of local error estimators and data approximation terms (see Theorem 6). The variational crimes introduced by the FE-HMM (the method is based on numerical quadrature) and the data approximation error (the data of the effective problem are unknown) are further analyzed (see Theorem 11).

The outline of this article is as follows. In Section 2 we briefly review the FE-HMM and the residual-based adaptive FE-HMM. In Section 3 we present the main results for the goal-oriented adaptive FE-HMM that are proved in Section 4. We show the efficiency and reliability of the method in various numerical experiments in Section 5. A summary of our main findings and outlook are given in the conclusion in Section 6.

Notation.. In what follows, $C > 0$ denotes a generic constant, independent of ε , whose value can change at any occurrence but depends only on the quantities which are indicated explicitly. For $r = (r_1, \dots, r_d) \in \mathbb{N}^d$, we denote $|r| = r_1 + \dots + r_d$, $D^r = \partial_1^{r_1} \dots \partial_d^{r_d}$. We will consider the usual Sobolev space $H^1(\Omega) = \{u \in L^2(\Omega); D^r u \in L^2(\Omega), |r| \leq 1\}$, with norm $\|u\|_{H^1(\Omega)} = (\sum_{|r| \leq 1} \|D^r u\|_{L^2(\Omega)}^2)^{1/2}$. We will also consider $H_0^1(\Omega)$ the closure of $C_0^\infty(\Omega)$ for the $\|\cdot\|_{H^1(\Omega)}$ norm and the spaces $W^{l,\infty}(\Omega) = \{u \in L^\infty(\Omega); D^r u \in L^\infty(\Omega), |r| \leq l\}$. For the unit cube $Y = (0, 1)^d$, we will consider $W_{per}^1(Y) = \{v \in H_{per}^1(Y); \int_Y v dx = 0\}$, where $H_{per}^1(Y)$ is defined as the closure of $C_{per}^\infty(Y)$ (the subset of $C^\infty(\mathbb{R}^d)$ of periodic functions in Y) in the H^1 norm. Finally, we will use the Frobenius matrix norm $\|a\|_F := \sqrt{\sum_i \sum_j |a_{ij}|^2}$.

2. Model problem and homogenization. We consider the elliptic problem with oscillatory coefficients in a domain $\Omega \subset \mathbb{R}^d$

$$\begin{aligned} -\nabla \cdot (a^\varepsilon \nabla u^\varepsilon) &= f && \text{in } \Omega, \\ u^\varepsilon &= g_D && \text{on } \partial\Omega, \end{aligned} \tag{2.1}$$

where we impose Dirichlet boundary conditions $g_D \in L^2(\partial\Omega)$ and $f \in L^2(\Omega)$. We emphasize the multiscale nature of the problem by using the superscript ε . We assume

that a^ε is symmetric, satisfies $a^\varepsilon(x) \in (L^\infty(\Omega))^{d \times d}$ and is uniformly elliptic and bounded, i.e.,

$$\exists \lambda, \Lambda > 0 \text{ such that } \lambda |\xi|^2 \leq a^\varepsilon(x) \xi \cdot \xi \leq \Lambda |\xi|^2, \quad \forall \xi \in \mathbb{R}^d \text{ and } \forall \varepsilon. \quad (2.2)$$

An application of the Lax-Milgram theorem ensures the existence of a family of solutions $\{u^\varepsilon\}$ that is bounded in $H_D^1(\Omega)$. From homogenization theory we know that there exists a symmetric tensor $a^0(x)$ and a subsequence of $\{u^\varepsilon\}$ that weakly converges to the so-called homogenized solution $u^0 \in H_D^1(\Omega)$ (we refer the reader to [23, 28, 44] and references therein). The proof relies on G-convergence [30] (or H-convergence [50]) and no further assumptions on the spatial structure of $a^\varepsilon(x)$ are needed for the weak convergence of a subsequence of $\{u^\varepsilon\}$. The homogenized solution u^0 solves a homogenized problem given by

$$\begin{aligned} -\nabla \cdot (a^0 \nabla u^0) &= f \quad \text{in } \Omega, \\ u^0 &= g_D \quad \text{on } \partial\Omega_D, \end{aligned} \quad (2.3)$$

where the homogenized tensor $a^0(x)$ is again symmetric and uniformly elliptic and bounded. Under the assumption that $a^\varepsilon(x) = a(x, x/\varepsilon)$ is periodic in its second argument, it can be shown that the whole sequence $\{u^\varepsilon\}$ weakly converges to $u^0 \in H_D^1(\Omega)$. In this case, we can also express the homogenized tensor $a^0(x)$ at a point $x \in \Omega$ in terms of solutions of d boundary value problems, the so-called cell problems. We remark that in general there are infinitely many cell problems to solve. For more general tensors a^ε , an explicit equation to compute the homogenized tensor at a point $x \in \Omega$ is not available. We therefore follow a numerical strategy, here the Finite Element Heterogeneous Multiscale Method (FE-HMM), in order to compute a numerically homogenized solution.

2.1. The Finite Element Heterogeneous Multiscale Method (FE-HMM).

We use the finite element heterogeneous multiscale method (FE-HMM) to obtain an approximation u^{HMM} to the homogenized (coarse) solution u^0 of (2.3) without computing the homogenized tensor $a^0(x)$ explicitly. We only need the oscillatory data $a^\varepsilon(x)$ to be given on sampling domains. The basic framework of the FE-HMM consists in a coupling of a macro problem and a micro problem, described below. For simplicity of presentation we will take zero Dirichlet boundary conditions in (2.1) and set $g_D = 0$.

Macro finite element space. We consider

$$V^p(\Omega, \mathcal{T}_H) = \{v^H \in H_0^1(\Omega); v^H|_K \in \mathcal{P}^p(K), \forall K \in \mathcal{T}_H\}, \quad (2.4)$$

with macro elements $K \in \mathcal{T}_H$, where \mathcal{T}_H is assumed to be shape regular. For simplicity, we only consider simplicial (triangular, tetrahedral) elements, but emphasize that other elements could also be used. Here \mathcal{P}^p is the space of piecewise polynomials on the element K of total degree p , and H is the size of the macro triangulation (notice that H can be much larger than ε).

Quadrature formulas. We consider for each macro element $K \in \mathcal{T}_H$ a C^1 -diffeomorphism F_K such that $K = F(\hat{K})$, where \hat{K} is a simplicial reference element. We consider a given quadrature formula (QF) $\{\hat{x}_\ell, \hat{\omega}_\ell\}_{\ell=1}^{\mathcal{L}}$ on the reference element \hat{K} ; the corresponding integration points on an element $K \in \mathcal{T}_H$ are given by $x_{K_\ell} = F_K(\hat{x}_\ell)$, $\ell = 1, \dots, \mathcal{L}$ and the corresponding quadrature weights on K are

given by $\omega_{K_\ell} = \hat{\omega}_\ell |\det(\partial F_K)|$, $\ell = 1, \dots, \mathcal{L}$. We make the following assumptions on the quadrature formulas (see [27]):

(Q1) $\hat{\omega}_j > 0$, $j = 1, \dots, J$, $\sum_{j=1}^J \hat{\omega}_j |\nabla \hat{p}(\hat{x}_j)|^2 \geq \hat{\lambda} \|\nabla \hat{p}\|_{L^2(\hat{K})}^2$, $\forall \hat{p}(\hat{x}) \in \mathcal{P}^\sigma(\hat{K})$, $\hat{\lambda} > 0$;

(Q2) $\int_{\hat{K}} \hat{p}(\hat{x}) d\hat{x} = \sum_{j=1}^J \hat{\omega}_j \hat{p}(\hat{x}_j)$, $\forall \hat{p}(\hat{x}) \in \mathcal{P}^\sigma(\hat{K})$. where $\sigma = \max(2p - 2, p)$.

REMARK 1. We notice here that the condition $\sigma = 1$ for \mathcal{P}^1 is needed in the FE-HMM for optimal macro L^2 bounds (see [5]). Such bounds will not be discussed here and in the sequel assumption **(Q2)** can be taken with $\sigma = 2p - 2$.

Macro bilinear form. For a discretization in the macro FE space (2.4) we define the FE-HMM bilinear form with $v^H, w^H \in V_D^p(\Omega, \mathcal{T}_H)$ as

$$B^{HMM}(v^H, w^H) = \sum_{K \in \mathcal{T}_H} \sum_{\ell=1}^{\mathcal{L}} \frac{\omega_{K_\ell}}{|K_{\delta_\ell}|} \int_{K_{\delta_\ell}} a^\varepsilon(x) \nabla v_{K_{\delta_\ell}}^h \cdot \nabla w_{K_{\delta_\ell}}^h dx, \quad (2.5)$$

where $v_{K_\ell}^h, w_{K_\ell}^h$ are appropriate micro functions defined on sampling domains K_{δ_ℓ} (see below) and the factor $|K_{\delta_\ell}|$ gives the appropriate weight for the contribution of the integrals defined on K_{δ_ℓ} instead of K . The FE-HMM bilinear form (2.5) is based by construction on numerical quadrature. Therefore, in our a posteriori analysis, we need to specially take care of the corresponding variational crimes.

Micro functions. For every macro element K we compute the solutions $v_{K_\ell}^h$ (and $w_{K_\ell}^h$) of micro problems on sampling domains K_{δ_ℓ} , $\ell = 1, \dots, \mathcal{L}$ within K . The contributions to the macro stiffness matrix are constructed from the micro functions given as follows: find $v_{K_\ell}^h$ such that $(v_{K_\ell}^h - v_{\text{lin}, K_\ell}^H) \in S^q(K_{\delta_\ell}, \mathcal{T}_h)$ and

$$\int_{K_{\delta_\ell}} a^\varepsilon(x) \nabla v_{K_\ell}^h \cdot \nabla z^h dx = 0 \quad \forall z^h \in S^q(K_{\delta_\ell}, \mathcal{T}_h), \quad (2.6)$$

where

$$v_{\text{lin}, K_\ell}^H(x) = v^H(x_{K_\ell}) + (x - x_{K_\ell}) \cdot \nabla v^H(x_{K_\ell}) \quad (2.7)$$

is a linearization of the macro function v^H at the integration point x_{K_ℓ} (see [34, 5] for details). The FE space is defined as

$$S^q(K_{\delta_\ell}, \mathcal{T}_h) = \{z^h \in W(K_{\delta_\ell}); z^h|_T \in \mathcal{P}^q(T), T \in \mathcal{T}_h\}, \quad (2.8)$$

where $W(K_{\delta_\ell})$ determines the coupling condition or boundary conditions used for computing the micro functions $v_{K_\ell}^h$ (or $w_{K_\ell}^h$).

Coupling micro and macro solvers. Several choices are possible for the coupling condition $(v_{K_\ell}^h - v_{\text{lin}, K_\ell}^H) \in S^q(K_{\delta_\ell}, \mathcal{T}_h)$ and we will consider $S^q(K_{\delta_\ell}, \mathcal{T}_h) \subset W(K_{\delta_\ell})$ with

$$W(K_{\delta_\ell}) = W_{\text{per}}^1(K_{\delta_\ell}) \quad (2.9)$$

for the periodic coupling and

$$W(K_{\delta_\ell}) = W_{\text{per}}^1(K_{\delta_\ell}) \quad (2.10)$$

for the Dirichlet coupling.

Variational problem. The macro solution of the FE-HMM is defined by the following variational problem: find $u^{HMM} \in V^p(\Omega, \mathcal{T}_H)$ such that

$$B^{HMM}(u^{HMM}, v^H) = \int_{\Omega} f v^H dx \quad \forall v^H \in V^p(\Omega, \mathcal{T}_H). \quad (2.11)$$

The main goal of the FE-HMM is to find a solution u^{HMM} that converges to the homogenized solution u^0 . Remember that the FE-HMM also depends on a micro mesh, thus h going to zero is also necessary for convergence (see Section 2.1.1). It can be shown that the FE-HMM bilinear form (2.5) is elliptic and bounded, i.e., it satisfies

$$B^{HMM}(v^H, v^H) \geq C \|v^H\|_{H^1(\Omega)}^2$$

and

$$|B^{HMM}(v^H, w^H)| \leq C \|v^H\|_{H^1(\Omega)} \|w^H\|_{H^1(\Omega)},$$

for all $v^H, w^H \in V^p(\Omega, \mathcal{T}_H)$ with a constant C that only depends on the quadrature formula, the domain Ω , the constant in (2.2). From the Lax-Milgram Theorem, existence and uniqueness of the solution u^{HMM} of problem (2.11) immediately follows (we refer to [1, 5, 34] for details).

2.1.1. A priori estimates. The sources of errors for the FE-HMM approximation to the homogenized solution can be decomposed as follows [1, 5, 6, 34]

$$\|u^0 - u^{HMM}\| \leq \|u^0 - u^{0,H}\| + \|u^{0,H} - \bar{u}^{HMM}\| + \|\bar{u}^{HMM} - u^{HMM}\|, \quad (2.12)$$

where the first term on the right-hand side of the above inequality represents the macro error, the second term represents the modeling error and the last term represents the micro error. Here, u^0 is the solution of (2.3), u^{HMM} is the FE-HMM solution of (2.11), $u^{0,H}$ is the FEM solution of the homogenized problem with numerical quadrature (using the same QF as for the HMM) of (2.3) in the space $V^p(\Omega, \mathcal{T}_H)$ and \bar{u}^{HMM} is the FE-HMM solution of (2.11) with exact micro functions (in $W(K_{\delta_\ell})$). The general form of the *a priori* error estimate in the H^1 -norm under the appropriate assumptions of $a^\varepsilon(x)$ is

$$\|u^0 - u^{HMM}\|_{H^1(\Omega)} \leq C(H^p + r_{MIC} + r_{MOD}), \quad (2.13)$$

where r_{MIC}, r_{MOD} are further described below. For the macro error CH^p , appropriate regularity of the homogenized tensor and homogenized solution is needed. For the micro error appropriate regularity of the tensor a^ε is needed. We briefly recall the assumption on the micro problem as this will be needed in this paper. Consider $\psi_{K_{\delta_\ell}}^{i,h}$, the solution of the following micro problem on the sampling domain K_{δ_ℓ}

$$\int_{K_{\delta_\ell}} a^\varepsilon(x) \nabla \psi_{K_{\delta_\ell}}^{i,h} \cdot \nabla z^h dx = - \int_{K_{\delta_\ell}} a^\varepsilon(x) \mathbf{e}_i \cdot \nabla z^h dx \quad \forall z^h \in S^q(K_{\delta_\ell}, \mathcal{T}_h), \quad (2.14)$$

where \mathbf{e}_i , $i = 1, \dots, d$, denote the canonical basis of \mathbb{R}^d .

We define on every macro quadrature point a numerically homogenized tensor denoted as $a_K^0(x_{K_\ell})$,

$$a_K^0(x_{K_\ell}) = \frac{1}{|K_{\delta_\ell}|} \int_{K_{\delta_\ell}} a^\varepsilon(x) \left(I + J_{\psi_{K_{\delta_\ell}}^h}(x) \right) dx, \quad (2.15)$$

where $J_{\psi_{K_{\delta_\ell}}^h}(x)$ is a $d \times d$ matrix whose entries are given by $\left(J_{\psi_{K_{\delta_\ell}}^h}(x) \right)_{ij} = (\partial \psi_{K_{\delta_\ell}}^{i,h}) / (\partial x_j)$.

Next, we introduce the tensor $\bar{a}_K^0(x_{K_\ell})$, which is defined as $a_K^0(x_{K_\ell})$ given in (2.15), but where the corresponding functions $\psi_{K_{\delta_\ell}}^i$ are found in the exact Sobolev space $W(K_{\delta_\ell})$ instead of its FE approximation $S^q(K_{\delta_\ell}, \mathcal{T}_h)$. Finally we will also consider for a sufficiently regular homogenized problem (see (2.3)), the homogenized tensor $a^0(x_{K_\ell})$ evaluated at the integration point x_{K_ℓ} . We can then express r_{MIC} and r_{MOD} in terms of the above tensors as follows

$$r_{MIC} := \sup_{K \in \mathcal{T}_H} \max_{1 \leq \ell \leq \mathcal{L}} \left\| \bar{a}_K^0(x_{K_\ell}) - a_K^0(x_{K_\ell}) \right\|_F, \quad (2.16)$$

$$r_{MOD} := \sup_{K \in \mathcal{T}_H} \max_{1 \leq \ell \leq \mathcal{L}} \left\| a^0(x_{K_\ell}) - \bar{a}_K^0(x_{K_\ell}) \right\|_F. \quad (2.17)$$

To estimate the micro error, we will need the following regularity assumption

(H1) Given $q \in \mathbb{N}$, the cell functions $\psi_{K_\ell}^i$ satisfy

$$|\psi_{K_\ell}^i|_{H^{q+1}(K_{\delta_\ell})} \leq C \varepsilon^{-q} \sqrt{|K_{\delta_\ell}|},$$

with C independent of $i = 1 \dots d$, ε , the quadrature point x_{K_ℓ} and the domain K_{δ_ℓ} .

We note that if $a_{ij}^\varepsilon|_K \in W^{1,\infty}(K) \forall K \in \mathcal{T}_H$ and $|a_{ij}^\varepsilon|_{W^{1,\infty}(K)} \leq C \varepsilon^{-1}$, then classical H^2 regularity results ([45, Chap. 2.6]) imply that $|\psi_{K_\ell}^i|_{H^2(K_{\delta_\ell})} \leq C \varepsilon^{-1} \sqrt{|K_{\delta_\ell}|}$ when Dirichlet boundary conditions $W(K_{\delta_\ell}) = H_0^1(K_{\delta_\ell})$ are used. If $a(x, x/\varepsilon) = a(x, y)$ is periodic in the y variable, then we can also use periodic boundary conditions $W(K_{\delta_\ell}) = H_{per}^1(K_{\delta_\ell})$, and higher regularity for $\psi_{K_\ell}^i$ can be shown, provided $a(x, \cdot)$ is smooth enough and $\delta/\varepsilon \in \mathbb{N}$ (see [24, Chap. 3]). We refer to [5, 6] for details.

Under assumption **(H1)**, the following estimate is valid [1, 6, 7]

$$r_{MIC} \leq C \left(\frac{h}{\varepsilon} \right)^{2q}, \quad (2.18)$$

where C is independent of H, h . Finally to estimate the modeling error, structure assumptions on the coefficients a^ε are needed.

(H2) $a^\varepsilon(x) = a(x, x/\varepsilon) = a(x, y)$ is Y -periodic in y ,

$$a_{ij}(x, y) \in \mathcal{C}(\bar{\Omega}; W_{per}^{1,\infty}(Y)), \text{ for all } i, j = 1, \dots, d.$$

Now if **(H2)** holds and if (2.6) is solved in $S^q(K_{\delta_\ell}, \mathcal{T}_h) \subset H_0^1(K_{\delta_\ell})$ with $\delta > \varepsilon$, then [34]

$$r_{MOD} \leq C \left(\frac{\varepsilon}{\delta} + \delta \right), \quad (2.19)$$

where C is independent of H and h .

Under the hypothesis **(H2)**, if the micro problems (2.6) are solved in $S^q(K_{\delta_\ell}, \mathcal{T}_h) \subset W_{per}^1(K_{\delta_\ell})$ with $\delta/\varepsilon \in \mathbb{N}$, and if the slow variable of the tensor $a(x, x/\varepsilon)$ is collocated at the quadrature points x_{K_ℓ} , i.e., $a(x_{K_\ell}, x/\varepsilon)$ in the problem (2.6) and in the bilinear form (2.5), then we have [13]

$$r_{MOD} = 0. \quad (2.20)$$

2.1.2. A posteriori error estimates for the FE-HMM. We recall the *a posteriori error* estimates for the FE-HMM following [10, 12, 6]. An important ingredient of the adaptive FE-HMM is the modeling of so-called multiscale fluxes (see (2.21)). For simplicity we consider here the piecewise linear case but emphasize that the energy-norm-based adaptive FE-HMM can be extended to higher order piecewise polynomials [53].

We first give the definition of the *jump of multiscale fluxes* (introduced in the context of the discontinuous Galerkin method in [4]), which is crucial for the error indicators used below. Let \mathcal{T}_H denote a conformal mesh and let \mathcal{E}_H be the set of interfaces. Two elements sharing an interface $e \in \mathcal{E}_H$ are labeled K^+ and K^- . Consider the micro functions $u_{K^+}^h$ and $u_{K^-}^h$ solutions of (2.6) in the two sampling domains K_δ^+ and K_δ^- of the elements K^+ and K^- , respectively, constrained by the macro solution u^{HMM} of (2.5).

DEFINITION 2 (Jump of multiscale fluxes).

$$\llbracket a^\varepsilon(x) \nabla u^h \rrbracket_e := \left(\frac{1}{|K_\delta^+|} \int_{K_\delta^+} a^\varepsilon(x) \nabla u_{K^+}^h dx - \frac{1}{|K_\delta^-|} \int_{K_\delta^-} a^\varepsilon(x) \nabla u_{K^-}^h dx \right) \cdot n_e, \quad (2.21)$$

for $e \not\subset \partial\Omega$ and $\llbracket a^\varepsilon(x) \nabla u^h \rrbracket_e := 0$ for $e \subset \partial\Omega$. In the above definition, the unit outward normal n_e is chosen to be $n_e = n^+$. We omit the index K_δ for the micro solutions u^h in $\llbracket a^\varepsilon(x) \nabla u^h \rrbracket_e$ as the jump over e involves two sampling domains in adjacent elements.

DEFINITION 3 (Local error indicator and data approximation error). *The local error indicator $\eta_H(K)$ on an element K is defined by*

$$\eta_H(K)^2 := H_K^2 \|f^H\|_{L^2(K)}^2 + \frac{1}{2} \sum_{e \subset \partial K} H_e \left\| \llbracket a^\varepsilon(x) \nabla u^h \rrbracket_e \right\|_{L^2(e)}^2. \quad (2.22)$$

The data approximation error $\xi_H(K)$ on an element K is defined by

$$\xi_H(K)^2 := H_K^2 \|f^H - f\|_{L^2(K)}^2 + \left\| \llbracket a^\varepsilon(x) \nabla u^h \rrbracket_e - a^0(x) \nabla u^{HMM} \right\|_{L^2(K)}^2, \quad (2.23)$$

where $a^0(x)$ is the unknown homogenized tensor of problem (2.3) and f^H is an approximation of f in the space $\{g^H \in L^2(\Omega); g^H|_K \in \mathcal{P}^0(K), \forall K \in \mathcal{T}_H\}$. The *a posteriori upper bound* for the error between the macroscopic FE-HMM solution u^H and the homogenized solution u^0 is given by

$$\|u^0 - u^{HMM}\|_{H^1(\Omega)}^2 \leq C \left(\eta_H(\Omega)^2 + \xi_H(\Omega)^2 \right)$$

and the *a posteriori lower bound* is given by

$$\eta_H(K)^2 \leq C \left(\|u^0 - u^{HMM}\|_{H^1(\omega_K)}^2 + \xi_H(\omega_K)^2 \right);$$

the upper and lower bounds have been derived in [10, 12]. Here the constant $C > 0$ depends only on the shape regularity constant γ , the coercivity and continuity bound (2.2), the dimension d and the domain ω_K consisting of all elements sharing at least one side with K .

We notice, as shown in [12], that the improvement in computational efficiency that is obtained by introducing adaptivity is even more significant for multiscale methods

than for single-scale methods. This is due to the fact that in a multiscale method, problems on both a microscopic and a macroscopic scale must be solved. In turn, by using adaptive mesh refinement, solutions of the problems on the microscopic scale may be re-used.

3. Adaptive goal-oriented error estimation for the FE-HMM. In this Section we construct macroscopic error estimators using an exact error representation of the error $e^H := u^0 - u^{HMM}$ in a quantity of interest, i.e.,

$$J(e^H) = J(u^0) - J(u^{HMM}),$$

where $J : V \rightarrow \mathbb{R}$ is a linear, bounded functional. We use the framework of the dual-weighted residual method that relies on a primal and a dual problem to extract the solution in the quantity of interest. Localized macroscopic refinement indicators are designed and used to drive an adaptive mesh refinement. These refinement indicators and error estimators depend on information from the microstructures that is recovered on the fly. We will sketch the relation between the microscopic averaging procedure used in the adaptive FE-HMM (such as the multiscale fluxes and jumps) and their equivalent classical, single-scale FEM counterparts.

3.1. Single-scale DWR FEM. The **primal problem** for the homogenized solution u^0 is given by (2.3), which reads in weak form

$$B_0(u^0, v) = \int_{\Omega} f v \, dx \quad \forall v \in H_0^1(\Omega). \quad (3.1)$$

Let $u^H \in V^p(\Omega, \mathcal{T}_H)$ be the FEM solution (without quadrature) of

$$B_0(u^H, v^H) = \int_{\Omega} f v^H \, dx \quad \forall v^H \in V^p(\Omega, \mathcal{T}_H). \quad (3.2)$$

By defining the dual solution $z^0 \in H_0^1(\Omega)$ given by

$$B_0(\varphi, z^0) = J(\varphi) \quad \forall \varphi \in H_0^1(\Omega), \quad (3.3)$$

we obtain that

$$J(u^0 - u^H) = B_0(u^0 - u^H, z^0). \quad (3.4)$$

As $z^0 \in H_0^1(\Omega)$ however is not available, we compute an approximation $z^{\mathcal{H}} \in V^{\mathcal{H}}$, where $V^{\mathcal{H}}$ is yet to be determined. Then we have that

$$J(u^0 - u^H) = B_0(u^0 - u^H, z^0) = \underbrace{B_0(u^0 - u^H, z^{\mathcal{H}})}_{=\eta_H(\Omega)} - \underbrace{B_0(u^0 - u^H, z^{\mathcal{H}} - z^0)}_{=\xi_H(\Omega)},$$

where $\eta_H(\Omega)$ is the error estimator and $\xi_H(\Omega)$ is the data approximation error. Due to Galerkin orthogonality, simply replacing z^0 by its discrete solution (without quadrature) $z^H \in V^p(\Omega, \mathcal{T}_H)$ and using the discrete primal solution u^H (without quadrature) will lead to $B_0(u^0 - u^H, z^H) = 0$. For the numerical approximation of z^0 , there are different strategies:

- Approximate the dual solution z^0 by the FEM solution $z^{\mathcal{H}}$ in a higher order polynomial space $V^{\mathcal{H}} := V^{\tilde{p}}(\Omega, \mathcal{T}_H)$ with $\tilde{p} > p$.

- Approximate the dual solution z^0 by higher-order interpolation based on the solution $z^H \in V^p(\Omega, \mathcal{T}_H)$. We refer to [20, 52, 61] for a discussion.
- Follow the h -approach and compute z^H in $V^{\mathcal{H}} := V^p(\Omega, \mathcal{T}_{\tilde{H}})$, where the triangulation $\mathcal{T}_{\tilde{H}}$ is obtained from \mathcal{T}_H by a suitable refinement of each element $K \in \mathcal{T}_{\tilde{H}}$ into finer subelements.

We also notice that due to Galerkin-orthogonality, equation (3.4) can be written as $J(u^0 - u^H) = B_0(u^0 - u^H, z^0) = B_0(u^0 - u^H, z^0 - \psi^H) \quad \forall \psi^H \in V^p(\Omega, \mathcal{T}_H)$. As we approximate the exact dual solution $z^0 \in V$ by $z^{\mathcal{H}} \in V^{\mathcal{H}}$, we will obtain a reliable method only if we can neglect the data approximation error $\xi_H(\Omega)$. It was shown by Nochetto et al. [52] that neglecting the approximation error can cause a severe underestimation of the error $J(e^H)$, even in rather simple examples, thus leading to an unreliable method. They further proposed a safeguarded DWR FEM method, which leads to unconditionally reliable enhanced estimators that asymptotically coincide with the original DWR method. We also mention the recent effort by Ainsworth and Rankin to develop guaranteed and fully computable bounds on the error in quantities of interest [15]. Finally, we remark that variational crimes, introduced by e.g., choosing the dual solution in the finite dimensional space $V^{\mathcal{H}}$ and using a bilinear form based on numerical quadrature are typically disregarded in the literature, even for the single-scale DWR FEM. As the FE-HMM is based by construction on numerical quadrature, we will have to analyze the corresponding variational crimes.

3.2. DWR FE-HMM. Inspired by the preceding discussion, we now define the DWR FE-HMM.

Primal problem. We approximate u^0 by the FE-HMM solution $u^{HMM} \in V^p(\Omega, \mathcal{T}_H)$, where u^{HMM} is the solution of

$$B^{HMM}(u^{HMM}, v^H) = \int_{\Omega} f v^H dx \quad \forall v^H \in V^p(\Omega, \mathcal{T}_H),$$

and where $B^{HMM}(\cdot, \cdot)$ refers to the FE-HMM bilinear form (2.5).

Dual problem. We choose the dual solution to be in the richer space

$$V^{\mathcal{H}} := V^{\tilde{p}}(\Omega, \mathcal{T}_H), \quad (3.5)$$

the FE space of piecewise polynomials of degree $\tilde{p} > p$. The discretized dual problem (using the FE-HMM) is then

$$B^{\mathcal{H}EMM}(\varphi^{\mathcal{H}}, z^{\mathcal{H}EMM}) = J(\varphi^{\mathcal{H}}) \quad \forall \varphi^{\mathcal{H}} \in V^{\tilde{p}}(\Omega, \mathcal{T}_H), \quad (3.6)$$

where $B^{\mathcal{H}EMM}(\cdot, \cdot)$ is the FE-HMM bilinear form (2.5) with an appropriate quadrature scheme (i.e., satisfying **(Q1)**, **(Q2)** for suitable higher order polynomials). We recall that we use the same family of triangulation \mathcal{T}_H for the primal and dual problems. The micro and modeling errors defined in (2.16), (2.17) will be denoted by r_{MIC} , r_{MOD} for the dual solution.

REMARK 4. *It is readily seen that the a priori estimates (2.13) for the macro error, (2.18) for the micro error and (2.19) for the modeling error are also valid for the dual solution $z^{\mathcal{H}EMM}$ under the same assumptions as for the primal solution u^{HMM} . In what follows, we assume that the same micro space $S^q(K_{\delta_\ell}, \mathcal{T}_h)$, the same family of micromeshes, and the same size of sampling domains are used for the primal and dual solutions. Thus the estimates (2.18), (2.19) (independent of the quadrature points) will be identical for u^{HMM} and $z^{\mathcal{H}EMM}$. In contrast, the estimates (2.16) or (2.17) may depend on the QF (that can be different for u^{HMM} or $z^{\mathcal{H}EMM}$).*

We briefly sketch how to extend the jump of multiscale fluxes defined in [12] for piecewise linear FEs to higher order polynomials. This is an important ingredient of the DWR-FE-HMM. We note that higher-order fluxes were first introduced in the context of the discontinuous Galerkin FE-HMM in [7].

Jumps of multiscale fluxes for higher order polynomials. Consider the higher order macro FE space $V^p(\Omega, \mathcal{T}_H)$. Then, for a given QF $\{x_{K_\ell}, \omega_{K_\ell}\}_{\ell=1}^{\mathcal{L}}$ that satisfies condition **(Q2)** (see Section 2.1), we have the following relation between the order of the FE space p and the number \mathcal{L} of nodes of the QF (see for example [59, Section 1])

$$\mathcal{L} \geq \frac{1}{2} p(p+1) \text{ for } d=2, \quad \mathcal{L} \geq \frac{1}{6} p(p+1)(p+2) \text{ for } d=3.$$

We consider quadrature formulae which minimize these inequalities in the following sense:

$$\begin{cases} \mathcal{L} = \frac{1}{2} p(p+1) & \text{for } d=2, \\ \mathcal{L} = \frac{1}{6} p(p+1)(p+2) & \text{for } d=3. \end{cases} \quad (3.7)$$

For a QF satisfying (3.7), we consider the following interpolation problem: for $v \in C^0(K)$ find $\Pi_v(x) \in \mathcal{P}^{p-1}(K)$ s.t.

$$\Pi_v(x_{K_\ell}) = v(x_{K_\ell}), \quad \ell = 1, \dots, \mathcal{L}, \quad (3.8)$$

where the interpolation nodes x_{K_ℓ} are given by the quadrature nodes of the QF $\{x_{K_\ell}, \omega_{K_\ell}\}_{\ell=1}^{\mathcal{L}}$. We then have the following lemma which is easy to prove (see [53] for details)

LEMMA 5. *Assume that **(Q2)** and (3.7) hold. Then, the interpolation problem (3.8) has a unique solution.* We emphasize that condition (3.7) is satisfied by various well-known QF (see e.g. [36, Chap. 8] or [63]). We refer the reader to [59] for a general discussion on the condition (3.7) and to [29] for an overview of the construction of cubature formulae. For the FE-HMM, it is strongly advised to choose such a QF, as it minimizes the number of quadrature points and therefore the number of micro problems needed to be solved for each macro element.

We now construct the higher-order multiscale fluxes based on the micro solutions at discrete points. We have \mathcal{L} micro solutions $v_{K_\ell}^h$ on the \mathcal{L} sampling domains K_{δ_ℓ} located around the quadrature nodes x_{K_ℓ} within the macro element K . Recall the numerically homogenized tensor $a_K^0(x_{K_\ell})$ defined in (2.15) for each sampling domain. The fluxes in the micro problems can be related to ‘‘macro fluxes’’ in the following sense (see [7, Corollary 5])

$$\frac{1}{|K_{\delta_\ell}|} \int_{K_{\delta_\ell}} a^\varepsilon(x) \nabla v_{K_\ell}^h dx = a_K^0(x_{K_\ell}) \nabla v^H(x_{K_\ell}), \quad \ell = 1, \dots, \mathcal{L}, \quad (3.9)$$

where $v_{K_\ell}^h$ is a solution of (2.6). On every macro element K we then define the interpolating polynomial $\Pi_{a^\varepsilon \nabla v_K^h}(x)$ in $(\mathcal{P}^{p-1}(K))^d$, which satisfies

$$\Pi_{a^\varepsilon \nabla v_K^h}(x_{K_\ell}) = \frac{1}{|K_{\delta_\ell}|} \int_{K_{\delta_\ell}} a^\varepsilon(x) \nabla v_{K_\ell}^h dx, \quad \ell = 1, \dots, \mathcal{L}. \quad (3.10)$$

We will refer to the interpolating polynomial $\Pi_{a^\varepsilon \nabla v_K^h}(x)$ as the *higher order multiscale flux*. Using (3.9) we see that

$$\Pi_{a^\varepsilon \nabla v_K^h}(x_{K_\ell}) = a_K^0(x_{K_\ell}) \nabla v^H, \quad \ell = 1, \dots, \mathcal{L}. \quad (3.11)$$

We further introduce for each interior interface e of two elements K^+ and K^- the following *jump of higher order multiscale fluxes*

$$\overline{[\Pi_{a^\varepsilon \nabla v_K^h}]_e}(s) := \begin{cases} \left(\Pi_{a^\varepsilon \nabla v_{K^+}^h}(s) - \Pi_{a^\varepsilon \nabla v_{K^-}^h}(s) \right) \cdot n_e & \text{for } e \not\subset \partial\Omega, \\ 0 & \text{for } e \subset \partial\Omega, \end{cases} \quad (3.12)$$

where the unit outward normal n_e is chosen to be $n_e = n^+$.

Exact error representation and data approximation error. We first define the interior and jump residuals that are used to express the exact error representation.

DEFINITION 6. *The interior and jump residuals $R_{I,H}$ in K and $R_{J,H}$ on e , are given, respectively, by*

$$\begin{aligned} R_{I,H}(x)|_K &= f^H + \nabla \cdot \left(\Pi_{a^\varepsilon \nabla u_K^h}(x) \right), \\ R_{J,H}(s)|_e &= -\frac{1}{2} \overline{[\Pi_{a^\varepsilon \nabla u_K^h}]_e}(s), \end{aligned}$$

where the multiscale flux $\Pi_{a^\varepsilon \nabla u_K^h}(x)$ is defined in (3.10) and the higher order jump of multiscale fluxes $\overline{[\Pi_{a^\varepsilon \nabla u_K^h}]_e}(s)$ is defined in (3.12). The local error estimator is defined by

$$\eta_H(K) := \int_K R_{I,H}(x) \left(z^{\mathcal{HMM}} - \psi^H \right) dx + \int_{\partial K} R_{J,H}(s) \left(z^{\mathcal{HMM}} - \psi^H \right) ds, \quad (3.13)$$

and the local refinement indicator is defined by

$$\bar{\eta}_H(K) := \left| \int_K R_{I,H}(x) \left(z^{\mathcal{HMM}} - \psi^H \right) dx + \int_{\partial K} R_{J,H}(s) \left(z^{\mathcal{HMM}} - \psi^H \right) ds \right|.$$

The function $\psi^H \in V^p(\Omega, \mathcal{T}_H)$ is an *arbitrary* function and we comment on this choice at the end of this subsection. As mentioned at the end of Section 3.1, variational crimes cannot be overlooked as the FE-HMM is based by construction on numerical quadrature. This leads to define the following data approximation error $\xi_H(K)$.

DEFINITION 7. *The data approximation error $\xi_H(K)$ on an element K is given by*

$$\xi_H(K) = \int_K \left(\Pi_{a^\varepsilon \nabla u_K^h}(x) - a^0(x) \nabla u^{\text{HMM}} \right) \cdot \nabla \left(z^{\mathcal{HMM}} - \psi^H \right) dx \quad (3.14a)$$

$$+ B_{0,K} \left(u^0 - u^{\text{HMM}}, z^0 - z^{\mathcal{HMM}} \right) \quad (3.14b)$$

$$+ B_{0,K} \left(u^0 - u^{\text{HMM}}, \psi^H \right) \quad (3.14c)$$

$$- \int_K (f^H - f) \left(z^{\mathcal{HMM}} - \psi^H \right) dx, \quad (3.14d)$$

where the subscript K in $B_{0,K}(\cdot, \cdot)$ indicates the restriction of $B_0(\cdot, \cdot)$ onto the element K and where f^H is an approximation of f in the space $\{g \in L^2(\Omega); g|_K \in$

$\mathcal{P}^m(K)$, $\forall K \in \mathcal{T}_H$ for $m \geq 0$. We will also define the global data approximation error by $\xi_H(\Omega) := \sum_{K \in \mathcal{T}_H} \xi_H(K)$. The components of the data approximation error (3.14) can be understood as follows: (3.14a) is the approximation error caused by using an inaccurate tensor (implicitly computed within the micro problem) and numerical quadrature instead of using the exact continuous $a^0(x)$ in the estimator; (3.14b) is the approximation error for using $z^{\mathcal{HMM}}$ instead of z^0 ; (3.14c) is the approximation error caused by the introduction of ψ^H and the lack of Galerkin orthogonality due to the discrepancy between u^{HMM} and u^H (u^H is the exact FEM solution without quadrature of problem (3.1)); finally, (3.14d) is the approximation error caused by approximating the right-hand side $f(x)$ in the estimator.

3.3. Main results. We can now state our first main result, the DWR FE-HMM error representation which will be proved in Section 4.

THEOREM 8 (Exact DWR FE-HMM error representation). *The error in quantities of interest is given by the exact representation*

$$J(u^0 - u^{\text{HMM}}) = \sum_{K \in \mathcal{T}_H} \eta_H(K) + \xi_H(K),$$

and the data approximation error $\xi_H(K)$ is specified in Definition 7. The DWR FE-HMM allows for cancelation of errors among elements; we therefore need to distinguish between the (global) signed error representation formula (Theorem 8) with local error estimators $\eta_H(K)$, and unsigned local refinement indicators $\bar{\eta}_H(K)$. The Theorem 8 and the Definition 6 immediately give the following results.

COROLLARY 9 (A posteriori DWR upper bound). *The following a posteriori upper bound holds*

$$|J(u^0 - u^{\text{HMM}})| \leq \sum_{K \in \mathcal{T}_H} \bar{\eta}_H(K) + |\xi_H(K)|. \quad (3.15)$$

REMARK 10. *As the refinement indicators $\bar{\eta}_H(K)$ are always positive we cannot, in general, find the optimal mesh which would take error cancelation among different elements into account. We remark that finding the optimal mesh is also not possible for the single-scale DWR FEM. While being not optimal, the mesh found using positive refinement indicators still leads to good convergence rates. However, the convergence curves might be very jagged instead of being a straight line. Our next main result (again proved in Section 4) gives an approximation of the data approximation error.*

THEOREM 11 (First estimation of the data approximation error). *Assume that (Q1), (Q2) hold with $\sigma = 2p - 2$ (primal solution) and $\sigma = 2\tilde{p} - 2$ (dual solution). Assume in addition that (3.7) hold for the primal solution, that the family of triangulation is shape regular and that for all $K \in \mathcal{T}_H$ the homogenized tensor $a^0(x)$ of problem (2.3) satisfies $a^0(x)|_K$ is constant. Then, the data approximation error $\xi_H(\Omega)$ can be estimated as follows*

$$\begin{aligned} |\xi_H(\Omega)| \leq & CH^{\tilde{p}} \left(H^{\tilde{p}} + \|\nabla \psi^H\|_{L^2(\Omega)} \right) + C \|f - f^H\|_{L^2(K)} \left\| \nabla \left(z^{\mathcal{HMM}} - \psi^H \right) \right\|_{L^2(\Omega)} \\ & + C (\bar{r}_{\text{MIC}} + \bar{r}_{\text{MOD}}) \left(H^p + (\bar{r}_{\text{MIC}} + \bar{r}_{\text{MOD}}) + \left\| \nabla \left(z^{\mathcal{HMM}} - \psi^H \right) \right\|_{L^2(\Omega)} \right), \end{aligned} \quad (3.16)$$

where $\bar{r}_{\text{MIC}} = \max\{r_{\text{MIC}}, r_{\text{MC}}\}$ and $\bar{r}_{\text{MOD}} = \max\{r_{\text{MOD}}, r_{\text{MD}}\}$ and where the constants C are independent of H, h and ε .

We notice that the assumption $a^0(x)|_K$ is constant in each $K \in \mathcal{T}_H$ is convenient to estimate the multiscale fluxes but could in principle be removed. This would however involve additional technicalities.

Several choices are possible for ψ^H . We consider two different choices, $\psi^H = 0$ and $\psi^H = z^{HMM}$, the dual solution $z^{HMM} \in V^p(\Omega, \mathcal{T}_H)$. Plugging $\psi^H = 0$ and $\psi^H = z^{HMM}$ in (3.16), and using the estimate (2.13) for z^{HMM} we obtain the following corollary of Theorem 11.

COROLLARY 12. *For $\psi^H = 0$ the data approximation error $\xi_H(\Omega)$ can be estimated as*

$$\begin{aligned} |\xi_H(\Omega)| &\leq CH^{p+\bar{p}} + C\|f - f^H\|_{L^2(K)} \\ &\quad + C\left(H^p + (\bar{r}_{MIC} + \bar{r}_{MOD}) + 1\right)(\bar{r}_{MIC} + \bar{r}_{MOD}), \end{aligned}$$

and for $\psi^H \equiv z^{HMM}$ as

$$\begin{aligned} |\xi_H(\Omega)| &\leq CH^p + C\left(H^p + (\bar{r}_{MIC} + \bar{r}_{MOD})\right)\|f - f^H\|_{L^2(K)} \\ &\quad + C\left(H^p + (\bar{r}_{MIC} + \bar{r}_{MOD})\right)(\bar{r}_{MIC} + \bar{r}_{MOD}). \end{aligned}$$

We emphasize that the error estimator of the DWR-FE-HMM method exploits cancellation of errors over different elements and we therefore expect the above estimates to significantly overestimate the real data approximation error.

We notice that Theorem 11 has been obtained without any specific regularity assumptions on the small scales or structure assumptions (e.g., periodicity) on the tensor a^ε . Such assumptions are however needed if we want to further estimate \bar{r}_{MIC} and \bar{r}_{MOD} as shown in the following result.

THEOREM 13 (Second estimation of the data approximation error). *If in addition to the assumptions of Theorem 11, the assumption **(H1)** holds then the estimation (3.16) is valid with $r_{MIC} \leq C\left(\frac{h}{\varepsilon}\right)^{2q}$. If further assumption **(H2)** holds, then r_{MOD} can be estimated as follows*

$$\begin{aligned} \bar{r}_{MOD} &= 0 && \text{if } S^q(K_{\delta_\ell}, \mathcal{T}_h) \subset W_{per}^1(K_{\delta_\ell}) \text{ and } \frac{\delta}{\varepsilon} \in \mathbb{N}, \\ \bar{r}_{MOD} &\leq C\left(\varepsilon + \left(\frac{\varepsilon}{\delta}\right)\right) && \text{if } S^q(K_{\delta_\ell}, \mathcal{T}_h) \subset H_0^1(K_{\delta_\ell}) \text{ } (\delta > \varepsilon). \end{aligned} \tag{3.17}$$

We next give a detailed description of the adaptive DWR FE-HMM that consists of loops of the form

$$\text{Solve} \rightarrow \text{Estimate} \rightarrow \text{Mark} \rightarrow \text{Refine}.$$

The detailed step-by-step procedure is given below.

ALGORITHM 14 (Adaptive DWR-FE-HMM).

Solve. *For the macro and micro meshes obtained by **REFINE**, compute the micro solutions (only for the refined macro elements) and the macro solutions u^{HMM} and z^{HMM} for the primal and the dual problem, respectively. Compute ψ^H if appropriate. Compute and store the higher-order multiscale fluxes $\Pi_{a^\varepsilon \nabla \varphi_K^h}(x)$ obtained by solving (2.14) constrained by the FE basis functions $\varphi^H \in V^p(\Omega, \mathcal{T}_H)$.*

Estimate. *Reconstruct the full multiscale fluxes $\Pi_{a^\varepsilon \nabla u_K^h}(x)$ and jumps*

$$\llbracket \Pi_{a^\varepsilon \nabla u_K^h} \rrbracket_e(s) \text{ (once } u^{HMM} \text{ is known). Estimate the error in the quantity}$$

of interest $J(u^0 - u^{HMM})$ by computing the estimate $\sum_{K \in \mathcal{T}_H} \eta_H(K)$ (this estimate can serve as a stopping criterion using $|\sum_{K \in \mathcal{T}_H} \eta_H(K)| < \text{tol}$, for a prescribed tolerance tol).

Mark. Mark the elements on a subset $\tilde{\mathcal{T}}_H$ of \mathcal{T}_H based on the refinement indicators $\bar{\eta}_H(K)$.

Refine. Refine the marked elements (and some neighbors for mesh conformity) and update the mesh for the primal and the dual problem. Update the micro meshes of the sampling domains corresponding to the refined macro elements (see below for a discussion about an optimal coupling).

REMARK 15. If a macro element is not marked for refinement, we carry over the solution of the corresponding microproblems from the current iteration to the next. This allows to significantly reduce the number of microproblems that need to be computed. We refer to [12, Section 4.1] for details.

In the residual-based adaptive FE-HMM case, the optimal coupling between the macro and micro mesh sizes for the data approximation error of the estimator is given – under appropriate assumptions – by $h_K \propto \varepsilon (H_K)^{\frac{p}{2q}}$. Here p and q refer to the polynomial degree of the (primal) macro and micro FE spaces, respectively [12]. Such *a priori* coupling conditions can be derived if we fix the way we measure the error (e.g., the energy norm for the residual-based adaptive FE-HMM). For error in quantities of interest, such coupling will depend on $J(\cdot)$, that is arbitrary (except for being linear and bounded). It would therefore be beneficial to introduce an a posteriori error estimator on the micro problems and couple the macro and micro refinement based on the experimental convergence rate of these error estimators.

As an alternative, a reduced basis technique could be used. There, a few representative basis functions with a large information content are computed once at an *offline* stage using a highly refined micro mesh. Typically, only a few reduced basis functions are needed if there is appropriate regularity with respect to the slow parameter. In the *online* stage, the reduced basis functions are used to approximate the solution of the micro problems with high accuracy, which renders an adaptive refinement of the micro meshes needless. We refer the reader to [8], where reduced basis combined with DWR-FE-HMM is studied.

4. Proofs of the main results. In this section we give the proof of Theorems 8 and 11. Our theoretical study will also allow to justify Definition 7 of the data approximation error.

Proof of Theorem 8 (Exact DWR FE-HMM error representation). We proceed in two steps. First, we use duality arguments to state the error in a quantity of interest that still depends on the unknown dual function z^0 . Second, we replace all numerically unavailable quantities, such as z^0, a^0 or f , by their computable, discrete approximations.

Step I. We want to find the exact error representation for the error $e^H := u^0 - u^{HMM}$ in the quantity of interest $J(\cdot)$, i.e.,

$$J(e^H) = J(u^0) - J(u^{HMM}).$$

The dual problem (3.3)

$$B_0(\varphi, z^0) = J(\varphi)$$

holds for all $\varphi \in H_0^1(\Omega)$. We therefore choose $\varphi = e^H$ to obtain

$$J(e^H) = B_0(e^H, z^0). \quad (4.1)$$

We next introduce an arbitrary $\psi^H \in V^p(\Omega, \mathcal{T}_H)$ in equation (4.1) and hence commit a variational crime as the FE-HMM solution is not computed with the bilinear form B_0 and therefore $B_0(e^H, \psi^H) \neq 0$. We have

$$\begin{aligned} & J(u^0 - u^{HMM}) \\ &= B_0(u^0 - u^{HMM}, z^0) \\ &= B_0(u^0 - u^{HMM}, z^0 - \psi^H) + B_0(u^0 - u^{HMM}, \psi^H). \end{aligned} \quad (4.2)$$

Step II. We next make the estimate computable. In (4.2), the dual solution z^0 is the exact solution of (3.3). Furthermore, the bilinear form $B_0(\cdot, \cdot)$ involves the exact homogenized tensor, and the primal solution u^0 of (3.1) depends on the exact right hand side f . As these quantities can in general not be evaluated exactly in the *a posteriori* error estimate, we replace them by computable quantities as follows.

We start by replacing the exact dual solution z^0 by the computable FE-HMM dual solution z^{HMM} in (4.2). We obtain

$$\begin{aligned} & J(u^0 - u^{HMM}) \\ &= B_0(u^0 - u^{HMM}, z^0 - \psi^H) + B_0(u^0 - u^{HMM}, \psi^H). \\ &= B_0(u^0 - u^{HMM}, z^{HMM} - \psi^H) + B_0(u^0 - u^{HMM}, z^0 - z^{HMM}) \\ &+ B_0(u^0 - u^{HMM}, \psi^H). \end{aligned} \quad (4.3)$$

The second and third terms of the right-hand side of (4.3) will be a contribution to the data approximation error. The first term of the right-hand side of (4.3) is further split into two parts,

$$\begin{aligned} B_0(u^0 - u^{HMM}, z^{HMM} - \psi^H) &= \int_{\Omega} f(z^{HMM} - \psi^H) dx \\ &- B_0(u^{HMM}, z^{HMM} - \psi^H), \end{aligned} \quad (4.4)$$

where we used (3.1). We replace the exact f in the first term of the right-hand of (4.4) by a computable approximation f^H and get

$$\int_{\Omega} f(z^{HMM} - \psi^H) dx = \int_{\Omega} f^H(z^{HMM} - \psi^H) dx - \int_{\Omega} (f^H - f)(z^{HMM} - \psi^H) dx. \quad (4.5)$$

We then substitute the flux $a^0 \nabla u^{HMM}(x)$ involving the exact homogenized tensor $a^0(x)$ by the computable multiscale flux (3.10) in the second term of the right-hand

of (4.4) and obtain

$$\begin{aligned}
& B_0 \left(u^{HMM}, z^{\mathcal{H}MM} - \psi^H \right) \\
&= \sum_{K \in \mathcal{T}_H} \int_K \left(a^0(x) \nabla u^{HMM} \right) \cdot \nabla \left(z^{\mathcal{H}MM} - \psi^H \right) dx \\
&= \sum_{K \in \mathcal{T}_H} \int_K \left(\Pi_{a^\varepsilon \nabla u_K^h}(x) \right) \cdot \nabla \left(z^{\mathcal{H}MM} - \psi^H \right) dx \\
&\quad - \sum_{K \in \mathcal{T}_H} \int_K \left(\Pi_{a^\varepsilon \nabla u_K^h}(x) - a^0(x) \nabla u^{HMM} \right) \cdot \nabla \left(z^{\mathcal{H}MM} - \psi^H \right) dx.
\end{aligned} \tag{4.6}$$

Finally, by integrating (4.6) by part we can separate the estimate into element terms and jump terms

$$\begin{aligned}
& B_0 \left(u^{HMM}, z^{\mathcal{H}MM} - \psi^H \right) \\
&= - \sum_{K \in \mathcal{T}_H} \int_K \nabla \cdot \left(\Pi_{a^\varepsilon \nabla u_K^h}(x) \right) \left(z^{\mathcal{H}MM} - \psi^H \right) dx \\
&\quad + \frac{1}{2} \sum_{K \in \mathcal{T}_H} \sum_{e \subset \partial K} \int_e \overline{\left[\Pi_{a^\varepsilon \nabla u_K^h} \right]}_e(s) \left(z^{\mathcal{H}MM} - \psi^H \right) ds \\
&\quad - \sum_{K \in \mathcal{T}_H} \int_K \left(\Pi_{a^\varepsilon \nabla u_K^h}(x) - a^0(x) \nabla u^{HMM} \right) \cdot \nabla \left(z^{\mathcal{H}MM} - \psi^H \right) dx,
\end{aligned} \tag{4.7}$$

where we used the definition of the jump of multiscale fluxes (3.12). We plug (4.4), (4.5) and (4.7) into (4.3) and obtain the error representation formula

$$J(u^0 - u^{HMM}) = \sum_{K \in \mathcal{T}_H} \eta_H(K) + \xi_H(K),$$

where $\eta_H(K)$ and $\xi_H(K)$ are defined in (3.13) and (3.14), respectively, and the proof is complete. \square

We remark that the integration by parts is not necessary, neither for the DWR FEM nor for the DWR FE-HMM. We integrate by parts solely to stay consistent with the results from the literature. We can as an alternative keep the original term in the right-hand side of (4.6), which may simplify the numerical evaluation.

Up to this point we did not assume specific regularity on the oscillating tensor, a^ε or make any spatial assumptions such as periodicity in the micro scale, to derive our error estimates. Furthermore, we kept both sampling domain size and boundary conditions of the micro problem for the FE-HMM rather general. We now find estimates of the data approximation error (3.14). Notice first that (see (3.11))

$$\left\| a^0(x) \nabla v^H - \Pi_{a^\varepsilon \nabla v_K^h}(x)(x) \right\|_{L^2(K)} = \left\| a^0(x) \nabla v^H(x) - \Pi_{a_K^0 \nabla v^H}(x) \right\|_{L^2(K)}.$$

Recalling the tensors a^0, \bar{a}_K^0 introduced in Section 2.1.1, we then consider the decom-

position

$$\begin{aligned} & \left\| a^0(x) \nabla v^H(x) - \Pi_{a_K^0 \nabla v^H}(x) \right\|_{L^2(K)} \leq \underbrace{\left\| a^0(x) \nabla v^H(x) - \Pi_{a^0 \nabla v_K^H}(x) \right\|_{L^2(K)}}_{e_I} \\ & + \underbrace{\left\| \Pi_{a^0 \nabla v_K^H}(x) - \Pi_{\bar{a}_K^0 \nabla v_K^H}(x) \right\|_{L^2(K)}}_{e_{II}} + \underbrace{\left\| \Pi_{\bar{a}_K^0 \nabla v_K^H}(x) - \Pi_{a_K^0 \nabla v_K^H}(x) \right\|_{L^2(K)}}_{e_{III}}, \end{aligned}$$

where $\Pi_{a^0(x_K) \nabla v_K^H}(x)$ and $\Pi_{\bar{a}_K^0 \nabla v_K^H}(x)$ are the interpolating polynomials based on the quadrature nodes $x_{K_\ell} \in K$ with function values given by $a^0(x_{K_\ell}) \nabla v^H(x_{K_\ell})$ and $\bar{a}_K^0(x_{K_\ell}) \nabla v^H(x_{K_\ell})$, respectively. The task is now to estimate e_I, e_{II}, e_{III} .

LEMMA 16. *Assume that **(Q2)** holds and that $a^0(x)|_K$ is constant in any $K \in \mathcal{T}_H$. Then*

$$e_I = 0.$$

The proof is trivial. Indeed, under the assumption of a locally constant homogenized tensor, the interpolation (3.10) is exact, i.e. $\Pi_{a^0 \nabla v_K^H}(x) \equiv a^0(x) \nabla v^H(x)$ for $x \in K$. Notice that in particular if hypothesis **(H2)** hold and if $a(\cdot, y)|_K$ is constant in each $K \in \mathcal{T}_H$, then the assumption of Lemma 16 is fulfilled.

To estimate e_{II} and e_{III} we need to relate the error of two interpolating polynomials to the error of the function values at the corresponding interpolation nodes. This relation will allow us to find similar estimates of the data approximation error as obtained in [12].

LEMMA 17. *For $v, \tilde{v} \in C^0(K)$ we consider the interpolation polynomials $\Pi_v(x) \in \mathcal{P}^{p-1}(K)$ and $\Pi_{\tilde{v}}(x) \in \mathcal{P}^{p-1}(K)$, respectively, defined by (3.8) based on the nodes of a QF $\{x_{K_\ell}, \omega_{K_\ell}\}_{\ell=1}^{\mathcal{L}}$ that satisfies **(Q2)** and (3.7). Then*

$$\|\Pi_v(x) - \Pi_{\tilde{v}}(x)\|_{L^2(K)} \leq C \sqrt{|K|} \max_{1 \leq \ell \leq \mathcal{L}} |v_\ell - \tilde{v}_\ell|,$$

where $|K|$ denotes the measure of the macro element K , the constant C only depends on the dimensionality d , the polynomial degree p , the shape regularity constant γ and the quadrature formula.

Proof. Using (3.8) we can introduce an interpolating polynomial $\Pi_{v-\tilde{v}}(x) \in \mathcal{P}^{p-1}(K)$ s.t. $\Pi_{v-\tilde{v}}(x_{K_\ell}) = v(x_{K_\ell}) - \tilde{v}(x_{K_\ell})$, $\ell = 1, \dots, \mathcal{L}$. We use the C^1 - diffeomorphism F_K between K and the reference element \hat{K} and define $\widehat{\Pi_{v-\tilde{v}}}(\hat{x}) := \Pi_{v-\tilde{v}}(F_K(\hat{x})) = \Pi_{v-\tilde{v}}(x)$. It is well-known that (see for example [25])

$$\|\Pi_{v-\tilde{v}}(x)\|_{L^2(K)} \leq C |\det(\partial F_K)|^{1/2} \left\| \widehat{\Pi_{v-\tilde{v}}}(\hat{x}) \right\|_{L^2(\hat{K})}. \quad (4.8)$$

Given a basis $\{\hat{q}_j\}_{j=1}^{\mathcal{L}}$ of $\mathcal{P}^{p-1}(\hat{K})$ we expand $\widehat{\Pi_{v-\tilde{v}}}(\hat{x}) = \sum_{j=1}^{\mathcal{L}} \hat{\beta}_j \hat{q}_j(\hat{x})$, with coefficients $\hat{\beta}_j \in \mathbb{R}$, $j = 1, \dots, \mathcal{L}$. Evaluating the above formula at $\hat{x}_\ell = F_K^{-1}(x_{K_\ell})$ we obtain $\widehat{\Pi_{v-\tilde{v}}}(\hat{x}_\ell) = \sum_{j=1}^{\mathcal{L}} \hat{A}_{\ell j} \hat{\beta}_j$, where $\hat{A}_{\ell j} = \hat{q}_j(\hat{x}_\ell)$. This last relation read in vector form $\hat{A} \hat{\beta} = \delta v$, where $(\hat{A})_{\ell j} = \hat{A}_{\ell j}$, $(\hat{\beta})_j = \hat{\beta}_j$ and $(\delta v)_\ell = v(x_{K_\ell}) - \tilde{v}(x_{K_\ell})$. From

Lemma 5 it follows that $\hat{\mathbf{A}}$ is invertible. Then we can estimate (4.8) further as follows

$$\begin{aligned}
\|\Pi_{v-\bar{v}}(x)\|_{L^2(K)} &\leq C |\det(\partial F_K)|^{1/2} \left\| \widehat{\Pi_{v-\bar{v}}}(\hat{x}) \right\|_{L^2(\hat{K})} \\
&\leq C \sqrt{|K|} \left\| \sum_{\ell=1}^{\mathcal{L}} \hat{\beta}_\ell \hat{q}_\ell(\hat{x}) \right\|_{L^2(\hat{K})} \\
&\leq C \sqrt{|K|} \sum_{\ell=1}^{\mathcal{L}} \|\hat{q}_\ell(\hat{x})\|_{L^2(\hat{K})} \|\hat{\beta}\|_\infty \\
&\leq C \sqrt{|K|} \left\| \hat{\mathbf{A}}^{-1}(\delta v) \right\|_\infty \leq C \sqrt{|K|} \max_{1 \leq \ell \leq \mathcal{L}} |v(x_{K_\ell}) - \bar{v}(x_{K_\ell})|,
\end{aligned}$$

where $\|\cdot\|_\infty$ is the supremum matrix and vector norm, respectively, and the constant C only depends on the dimensionality d , the polynomial degree p , the shape regularity constant γ , the quadrature formula $\{\hat{x}_\ell, \hat{\omega}_\ell\}_{\ell=1}^{\mathcal{L}}$ and the basis $\{\hat{q}_j\}_{j=1}^{\mathcal{L}}$ of $\mathcal{P}_d^{p-1}(\hat{K})$. \square We can next relate the modeling and the micro errors to the various numerically homogenized tensors.

LEMMA 18. *Assume that (Q1) holds and that the family of triangulation is shape regular, then we have*

$$e_{II} \leq C \max_{1 \leq \ell \leq \mathcal{L}} \|a^0(x_{K_\ell}) - \bar{a}_K^0(x_{K_\ell})\|_F \|\nabla v^H(x)\|_{L^2(K)}, \quad (4.9)$$

and

$$e_{III} \leq C \max_{1 \leq \ell \leq \mathcal{L}} \|\bar{a}_K^0(x_{K_\ell}) - a_K^0(x_{K_\ell})\|_F \|\nabla v^H(x)\|_{L^2(K)}, \quad (4.10)$$

where the constant C only depends on the dimensionality d , the polynomial degree p of the FEM for u^H , the shape regularity constant and the quadrature formula.

Proof. Both estimates use Lemma 17. For example for e_{II} we have

$$\begin{aligned}
e_{II} &= \left\| \Pi_{a^0 \nabla v_K^H}(x) - \Pi_{\bar{a}_K^0 \nabla v_K^H}(x) \right\|_{L^2(K)} \\
&\leq C \sqrt{|K|} \max_{1 \leq \ell \leq \mathcal{L}} \|(a^0(x_{K_\ell}) - \bar{a}_K^0(x_{K_\ell})) \nabla v^H(x_{K_\ell})\|_\infty \\
&\leq C \left(\max_{1 \leq \ell \leq \mathcal{L}} \|(a^0(x_{K_\ell}) - \bar{a}_K^0(x_{K_\ell}))\|_F \right) \sum_{\ell=1}^{\mathcal{L}} \sqrt{|K|} \left(\sum_j \partial_j v^H(x_{K_\ell})^2 \right)^{1/2} \\
&\leq C \left(\max_{1 \leq \ell \leq \mathcal{L}} \|a^0(x_{K_\ell}) - \bar{a}_K^0(x_{K_\ell})\|_F \right) \|\nabla v^H(x)\|_{L^2(K)}, \quad (4.11)
\end{aligned}$$

where we used that

$$\sum_{\ell=1}^{\mathcal{L}} \sqrt{|K|} \left(\sum_j \partial_j v^H(x_{K_\ell})^2 \right)^{1/2} \leq C \left(\sum_{\ell=1}^{\mathcal{L}} \omega_{K_\ell} \sum_j \partial_j v^H(x_{K_\ell})^2 \right)^{1/2} \quad (4.12)$$

$$\leq C \|\nabla v^H(x)\|_{L^2(K)}. \quad (4.13)$$

This last inequalities are obtained using the assumption (Q1), a scaling argument as well as the equivalence of norms on a finite dimensional space (see for example [58,

Lemma 5]). The proof of (4.10) is obtained similarly. \square

Proof of Theorem 11 (First estimation of the data approximation error). Summing over the local data approximation error defined in (3.14) gives

$$\begin{aligned}
\sum_{K \in \mathcal{T}_H} \xi_H(K) &= \underbrace{\sum_{K \in \mathcal{T}_H} \int_K \left[\Pi_{a^\varepsilon \nabla u_K^h}(x) - a^0(x) \nabla u^{HMM} \right] \cdot \nabla \left(z^{\mathcal{HMM}} - \psi^H \right) dx}_I \\
&+ \underbrace{\sum_{K \in \mathcal{T}_H} B_{0,K} \left(u^0 - u^{HMM}, z^0 - z^{\mathcal{HMM}} \right)}_{II} \\
&+ \underbrace{\sum_{K \in \mathcal{T}_H} B_{0,K} \left(u^0 - u^{HMM}, \psi^H \right)}_{III} \\
&+ \underbrace{\sum_{K \in \mathcal{T}_H} \int_K (f - f^H) \left(z^{\mathcal{HMM}} - \psi^H \right) dx}_{IV}. \tag{4.14}
\end{aligned}$$

In view of the definitions (2.16) and (2.17) for r_{MIC} and r_{MOD} , respectively, we have

$$|I| \leq C (r_{MIC} + r_{MOD}) \left\| \nabla z^{\mathcal{HMM}} - \nabla \psi^H \right\|_{L^2(\Omega)}$$

where we used Lemmas 16 and 18, the Cauchy-Schwarz inequality and the bound $\|\nabla u^H\|_{L^2(\Omega)} \leq C \|f\|_{L^2(\Omega)} \leq C$. Using Cauchy-Schwarz inequality we obtain

$$\begin{aligned}
|II| &\leq C \left\| \nabla u^0 - \nabla u^{HMM} \right\|_{L^2(\Omega)} \left\| \nabla z^0 - \nabla z^{\mathcal{HMM}} \right\|_{L^2(\Omega)} \\
&\leq (H^p + r_{MIC} + r_{MOD}) (H^{\tilde{p}} + r_{MIC} + r_{MOD}).
\end{aligned}$$

and similarly

$$|III| \leq C (H^p + r_{MIC} + r_{MOD}) \left\| \nabla \psi^H \right\|_{L^2(\Omega)},$$

$$|IV| \leq C \|f - f^H\|_{L^2(\Omega)} \left\| \nabla z^{\mathcal{HMM}} - \nabla \psi^H \right\|_{L^2(\Omega)}.$$

We use $\bar{r}_{MIC} = \max\{r_{MIC}, r_{MIC}\}$ and $\bar{r}_{MOD} = \max\{r_{MOD}, r_{MOD}\}$ and conclude the proof of (3.16) by noting that the polynomial degree of the dual solution satisfies $\tilde{p} > p$. \square

Proof of Theorem 13 (Second estimation of the data approximation error). The proof of the theorem follows from (3.16) using the estimate (2.18) under assumption **(H1)**, and the estimates (2.20),(2.19) under assumption **(H2)** with the appropriate finite element spaces. \square

5. Numerical experiments . In this section we will show numerical experiments that confirm the efficiency of the goal-oriented, adaptive FE-HMM and the effectivity of the estimated error in a quantity of interest. Our numerical experiments

were carried out using an implementation in Matlab; this implementation is based on the FE-HMM code presented in [11]. The code for the mesh bisection is based in part on *i*FEM (see [26]) and the code for higher-order FEM is based in part on [21].

We consider a problem (which is chosen similarly to the one-dimensional problems presented in [57]) where we are interested in the pointwise error and the pointwise directional derivative error at a certain point x^* . We consider the equation

$$\begin{aligned} -\nabla \cdot (a^\varepsilon(x) \nabla u^\varepsilon) &= f \text{ in } \Omega, \\ u^\varepsilon &= g_D \text{ on } \Gamma_D = \partial\Omega, \end{aligned}$$

on a domain $\bar{\Omega} = (0, 1)^2$. We choose $\varepsilon = 10^{-5}$ and set the tensor to

$$a\left(x, \frac{x}{\varepsilon}\right) := \tilde{a}^\varepsilon\left(\frac{x}{\varepsilon}\right) a^0(x),$$

where the exact homogenized tensor $a^0(x)$ is given as

$$a^0(x) := \left(9e^{-1000(x_1-0.5)^2-1000(x_2-0.5)^2} + 1\right) I_2. \quad (5.1)$$

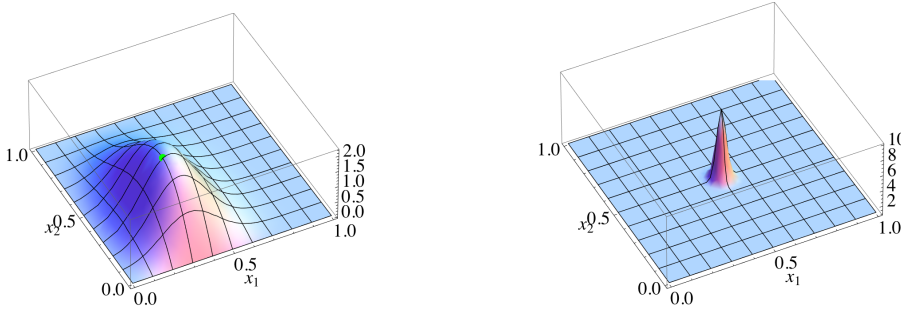
Here

$$\tilde{a}^\varepsilon(x) := \frac{16}{15} \left(\sin\left(2\pi \frac{x_1}{\varepsilon}\right) + \frac{5}{4} \right) \left(\cos\left(2\pi \frac{x_2}{\varepsilon}\right) + \frac{5}{4} \right),$$

whose coefficients are chosen in such a way that they give the unit tensor when homogenized. We define the exact solution as

$$u^0(x) := 100(1-x_1)^2 x_1 (1-x_2)^2 x_2 e^{-20(x_1-\frac{1}{3})^2 - (x_2-\frac{1}{4})^2},$$

which determines the Dirichlet boundary conditions as $g_D = u^0$ on $\partial\Omega$, and choose the right hand side f accordingly. An illustration of the exact solution and the



(a) Exact homogenized solution $u^0(x)$. We are interested in the pointwise error and the directional derivative error at the point $x^* = (0.3, 0.3)$, which is marked in green.

(b) Exact homogenized tensor $a^0(x)$.

Fig. 5.1: Exact solution and tensor of the goal-oriented problems of Section 5.

homogenized tensor are given in Figure 5.1. We use piecewise linear macro FE for

the solution u^{HMM} of the primal problem and piecewise quadratic FE for the solution z^{HMM} of the macro dual problem. The micro problems are solved with piecewise linear FE.

As a measure of the quality of our error estimator, we define the effectivity index

$$\text{Eff} := \left| \frac{\eta_H(\Omega)}{J(u^0 - u^{HMM})} \right|, \quad (5.2)$$

which ideally should be equal to one. We denote by $\hat{h} := (N_{mic})^{-1/d}$ the scaled (i.e. independent of ε) micro mesh size, where N_{mic} refers to the degrees of freedom of the micro problems in one micro sampling domain corresponding to a certain macro element.

For the macro mesh we start for both problems from a mesh with 441 DOF. We do not choose a uniform grid but one where the points are slightly distorted compared to uniform mesh, see Figure 5.7. The distortion will resemble to more realistic meshes originating from practical applications and reduce effects of cancellation. We use an initial mesh size for the micro mesh of $\hat{h} = \frac{1}{8}$ and $\delta = \varepsilon = 10^{-5}$ with periodic boundary conditions for the micro problems.

For the marking strategy we will follow the *maximum marking strategy* [60, 57] for the quantity of interest $J(u^0 - u^{HMM})$. An element K of the mesh is refined if

$$\frac{\tilde{\eta}_H(K)}{\max_{\tilde{K} \in \mathcal{T}_H} \tilde{\eta}_H(\tilde{K})} \geq \vartheta,$$

where $0 < \vartheta < 1$ is a user-defined parameter. We choose $\vartheta = 0.25$. The mesh is refined using the newest vertex bisection in its implementation of *iFEM* [26]. We remark that we do not enforce the creation of an interior node as mentioned in [49].

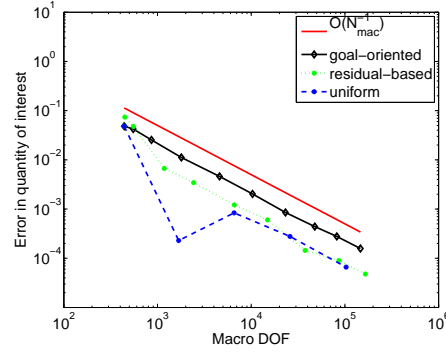
We set $\psi^H \equiv 0$ and choose a coupling of $\hat{h} \propto H_k$ for both the solution of the primal and dual problem and for the evaluation of the *a posteriori* estimator. For numerical experiments with different ψ^H or coupling schemes, we refer to [53].

We recall that for macro elements that were not refined, the solution of the micro-problems from the previous iteration should be re-used (see Remark 15).

5.1. Pointwise error. In our first experiment, we choose the quantity of interest to be the pointwise error at the point $x^* = (0.3, 0.3)$; the quantity of interest is

$$J(u) := u(x^*).$$

The point x^* coincides with a node of the mesh and the exact quantity of interest is given by $J(u) \approx 2.10813$. In Figure 5.2 we compare the error for the uniform refinement, the global residual-based refinement and the goal-oriented refinement of the FE-HMM. The error of all three methods shows an asymptotic convergence rate of $\mathcal{O}(N_{mac}^{-1})$. The pointwise error is smaller for the uniform or residual-based adaptivity than it is for the goal-oriented adaptivity. But the DWR FE-HMM also provides an estimation of the actual error in the quantity of interest, which serves as a stopping criterion. In Figure 5.3 we present the effectivity index for the residual-based adaptivity and the goal-oriented adaptivity. While the effectivity index for goal-oriented adaptivity is close to one, the residual-based estimate approximates the error in the

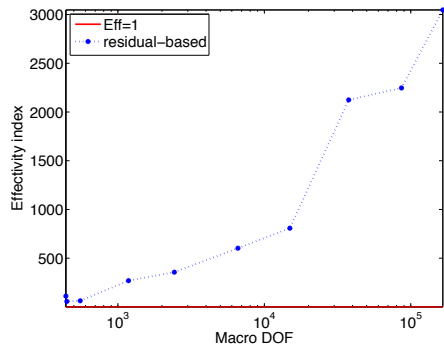


(a) Error for uniform, global residual-based and goal-oriented refinement.

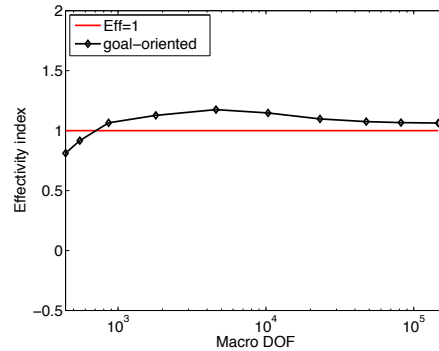
Fig. 5.2: Errors for the goal-oriented problem described in Section 5.1.

energy norm and therefore gives an effectivity index which is not suitable as a stopping criterion; the residual-based error estimate further depends on an unspecific constant. In the first two iterations for the DWR FE-HMM, the error is underestimated, leading to an effectivity index smaller than one. Additional *a posteriori* error estimates on the different components of the data approximation error can be used to avoid the underestimation of the error, we refer to [15, 52] and to the comment at the end of Section 3.3.

Finally, we compare in Figure 5.4 the mesh of the goal-oriented and the residual-based adaptivity after 4 iterations. We see that the mesh is highly refined around x^* and the “peak” of the tensor for the goal-oriented adaptivity, whereas the residual-based adaptivity obviously does not especially refine around x^* .



(a) Effectivity index for the global residual-based $(\frac{\eta_{H,Residual}(\Omega)}{|J(e^H)|})$ and goal-oriented adaptivity.



(b) Effectivity index for the goal-oriented adaptivity.

Fig. 5.3: Effectivity index for the goal-oriented problem described in Section 5.1.

5.2. Pointwise directional derivative error. We choose our quantity of interest to be the directional derivative error at the point $x^* = (0.3, 0.3)$ (slightly off the peak of the “bump”) in direction $n = (1/\sqrt{2}, 1/\sqrt{2})$, such that

$$J(u) := \nabla u(x^*) \cdot n. \quad (5.3)$$

The exact solution is given by $J \approx 3.25819$. As the pointwise derivatives of FE solutions are in general not defined on edges of elements, we approximate the functional (5.3) at point $x^* \in \Omega$ with a regularized output functional $J(u) = \frac{1}{|S^\epsilon|} \int_{S^\epsilon} \nabla u \cdot n \, dx$, where the small domain S^ϵ is an ϵ -ball centered around the point x^* , see [20]. In

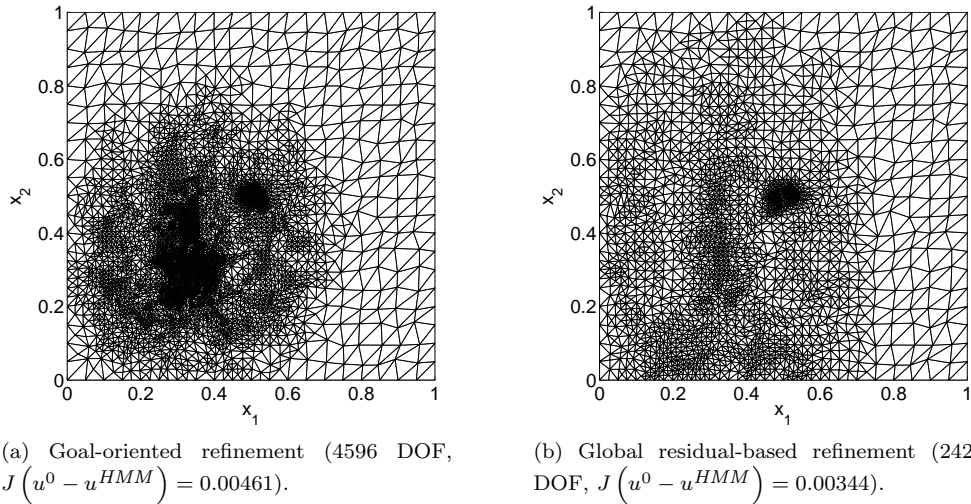
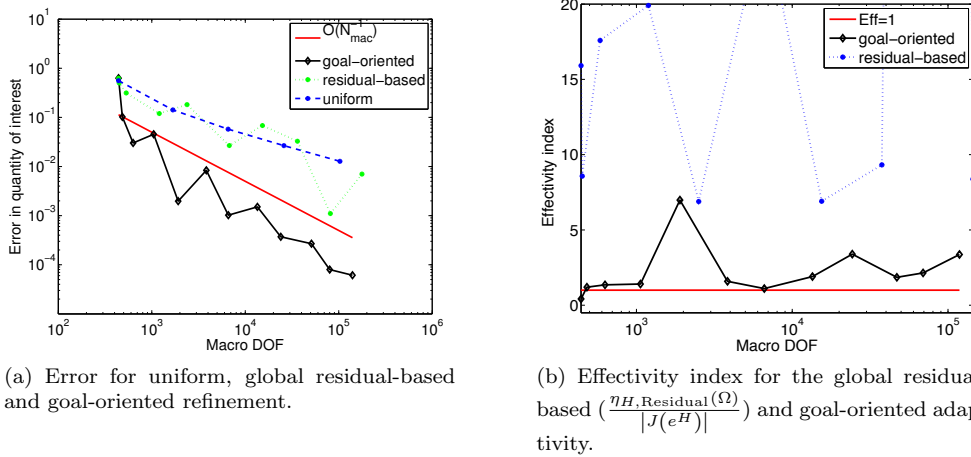


Fig. 5.4: Mesh after 4 iterations for global residual-based and goal-oriented refinement for the pointwise directional derivative problem.

Figure 5.5(a) we compare the error when using a uniform, a global residual-based (as in [12]) and the DWR FE-HMM goal-oriented approach. We see that the pointwise derivative error $J(e^H)$ converges with an order of $\mathcal{O}(N_{mac}^{-1/2})$ for the uniform refinement and for the adaptive, residual-based refinement scheme. For the DWR FE-HMM we obtain a (mean) convergence rate of approximately $\mathcal{O}(N_{mac}^{-3/2})$, which varies between $\mathcal{O}(N_{mac}^{-1})$ and $\mathcal{O}(N_{mac}^{-2})$. We notice that the convergence rate is much faster than the $\mathcal{O}(N_{mac}^{-1/2})$ we would have in the global energy-norm. In Figure 5.5(b) we see that the effectivity index for the DWR FE-HMM varies between 0.5 and 8. The residual-based estimate in the energy norm involves an unspecific constant, varies between 7 and 120 and is not suitable for estimating the error in the quantity of interest. Therefore the residual-based estimate is also unsuitable as a reliable stopping criterion. The jagged line for the error and efficiency of the DWR FE-HMM is caused by the cancellation of errors; the jaggedness can also be seen in the single-scale DWR FEM case.

We illustrate in Figure 5.6 how the dual-weighted residual error estimates can be used to evaluate the quality of the numerical solution. As the exact error represen-

tation does not involve an unspecific constant, we have the possibility to specify – solely based on the error estimate – a *confidence interval* where we expect the exact quantity of interest to be. If the data approximation error is much smaller than the error estimator $\eta_H(\Omega)$, we can set $J(u^{HMM}) - |\eta_H(\Omega)|$ and $J(u^{HMM}) + |\eta_H(\Omega)|$ to be our confidence interval. We see in Figure 5.6 that except for iteration 1, the exact solution lies within the confidence interval.



(a) Error for uniform, global residual-based and goal-oriented refinement.

(b) Effectivity index for the global residual-based ($\frac{\eta_{H, \text{Residual}}(\Omega)}{|J(e^H)|}$) and goal-oriented adaptivity.

Fig. 5.5: Errors and effectivity index for the goal-oriented problem described in Section 5.2.

Finally we show in Figure 5.7 the meshes after 4 iterations for both the goal-oriented and the residual-based adaptive FE-HMM. While the residual-based scheme mostly refines around the peak of the conductivity tensor, the goal-oriented additionally refines around the point of interest x^* .

6. Conclusion. We have presented an *a posteriori* error analysis in quantities of interest for the FE-HMM and generalized the DWR approach for homogenization problems. An exact error representation has been derived and effective error indicators have been modeled based solely on micro computations on sampling domains within the physical computational domain. Rigorous upper bound on the data approximation errors have been established. These errors also take into account the variational crimes committed by our computational strategy relying on numerical integration. Numerical experiments presented in the present paper confirm the efficiency of the proposed (multiscale) adaptive method in quantity of interests. We note that even for single scale problems, the DWR for FEM with numerical integration has not yet been analyzed. While we have provided an *a priori* upper bound for the data approximation error we did not provide an *a posteriori* error estimate for these quantities. This could be addressed by designing also an *a posteriori* error procedure for the micro solution in the sampling domains. Such an *a posteriori* error estimate on the micro solutions could also be used to find a suitable coupling condition between the macro and the

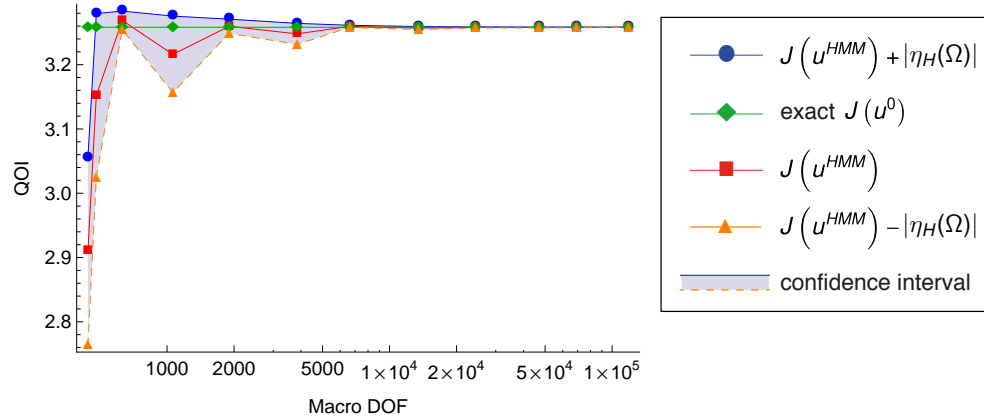
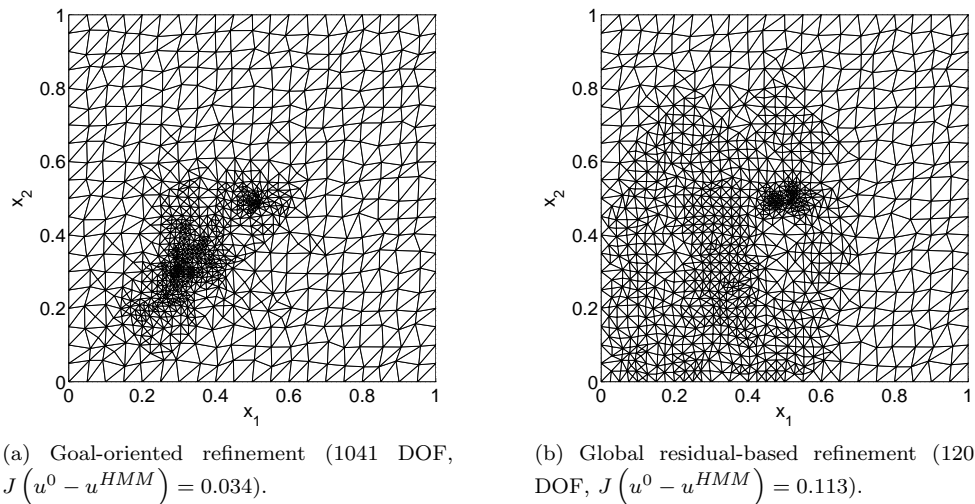


Fig. 5.6: The use of duality-based goal-oriented FE-HMM allows to specify – solely based on the *a posteriori* error estimate – a *confidence interval* (shown in shaded blue) where we expect the exact quantity of interest to be within. From iteration 2 on, the prediction is correct.



(a) Goal-oriented refinement (1041 DOF, $J(u^0 - u^{HMM}) = 0.034$).

(b) Global residual-based refinement (1209 DOF, $J(u^0 - u^{HMM}) = 0.113$).

Fig. 5.7: Mesh after 4 iterations for global residual-based and goal-oriented refinement for the pointwise directional derivative problem.

micro problems for general quantities of interest. For single scale problems, in the conforming case, *a posteriori* bounds for the data approximation errors were recently derived in [15]. For multiscale problems as considered here and with the proposed micro-to-macro approach, quantifying the modeling error and the error arising from variational crimes would also be required. This is a topic for future research.

REFERENCES

- [1] A. Abdulle. On A Priori Error Analysis of Fully Discrete Heterogeneous Multiscale FEM. *SIAM Multiscale Modeling & Simulation*, 4(2):447–459, 2005.
- [2] A. Abdulle. Analysis of a Heterogeneous Multiscale FEM for Problems in Elasticity. *Math. Mod. Meth. Appl. Sci. (M3AS)*, 6:615–635, 2006.
- [3] A. Abdulle. Heterogeneous multiscale method with quadrilateral elements. *Numerical mathematics and advanced applications*, Springer, Berlin, pages 743–751, 2006.
- [4] A. Abdulle. Multiscale method based on discontinuous Galerkin methods for homogenization problems. *Comptes rendus-Mathématique*, 346(1-2):97–102, 2008.
- [5] A. Abdulle. The finite element heterogeneous multiscale method: a computational strategy for multiscale PDEs. *GAKUTO International Series, Math. Sci. Appl.*, 31:135–181, 2009.
- [6] A. Abdulle. A priori and a posteriori error analysis for numerical homogenization: a unified framework. *Ser. Contemp. Appl. Math. CAM*, 16:280–305, 2011.
- [7] A. Abdulle. Discontinuous Galerkin Finite Element Heterogeneous Multiscale Method for Elliptic Problems with Multiple Scales. *To appear in Math. Comp.*, 2012.
- [8] A. Abdulle and Y. Bai. A reduced basis heterogeneous multiscale method. *submitted for publication*, 2011.
- [9] A. Abdulle and B. Engquist. Finite element heterogeneous multiscale methods with near optimal computational complexity. *SIAM Multiscale Modeling & Simulation*, 6(4):1059–1084, 2007.
- [10] A. Abdulle and A. Nonnenmacher. A posteriori error analysis of the heterogeneous multiscale method for homogenization problems. *Comptes Rendus Mathématique*, 347(17-18):1081–1086, 2009.
- [11] A. Abdulle and A. Nonnenmacher. A short and versatile finite element multiscale code for homogenization problems. *Computer Methods in Applied Mechanics and Engineering*, 198(37-40):2839–2859, 2009.
- [12] A. Abdulle and A. Nonnenmacher. Adaptive finite element heterogeneous multiscale method for homogenization problems. *Computer Methods in Applied Mechanics and Engineering*, 200:2710–2726, 2011.
- [13] A. Abdulle and Ch. Schwab. Heterogeneous Multiscale FEM for Diffusion Problems on Rough Surfaces. *SIAM Multiscale Modeling & Simulation*, 3(1):195–220, 2005.
- [14] M. Ainsworth and J.T. Oden. A posteriori error estimation in finite element analysis. *Computer Methods in Applied Mechanics and Engineering*, 142(1-2):1–88, 1997.
- [15] M. Ainsworth and R. Rankin. Guaranteed computable bounds on quantities of interest in finite element computations. *submitted to the International Journal of Numerical Methods in Engineering*, 2011.
- [16] I. Babuška, G. Caloz, and J.E. Osborn. Special finite element methods for a class of second order elliptic problems with rough coefficients. *SIAM Journal on Numerical Analysis*, 31(4):945–981, 1994.
- [17] I. Babuška and J.E. Osborn. Generalized finite element methods: their performance and their relation to mixed methods. *SIAM Journal on Numerical Analysis*, 20(3):510–536, 1983.
- [18] I. Babuška and W.C. Rheinboldt. Error estimates for adaptive finite element computations. *SIAM Journal on Numerical Analysis*, 15(4):736–754, 1978.
- [19] I. Babuška and T. Strouboulis. *The finite element method and its reliability*. Oxford University Press, USA, 2001.
- [20] W. Bangerth and R. Rannacher. *Adaptive Finite Element Methods for Differential Equations*. Birkhäuser Verlag, Basel, 2003.
- [21] S. Bartels, C. Carstensen, and A. Hecht. P2Q2Iso2D= 2D isoparametric FEM in Matlab. *Journal of Computational and Applied Mathematics*, 192(2):219–250, 2006.
- [22] R. Becker and R. Rannacher. An optimal control approach to a posteriori error estimation in finite element methods. *Acta numerica*, 10:1–102, 2001.
- [23] A. Bensoussan, J.L. Lions, and G. Papanicolaou. *Asymptotic analysis for periodic structures (Studies in mathematics and its applications)*. Elsevier North-Holland, 1978.
- [24] L. Bers, F. John, and M. Schechter. Partial differential equations. *Lectures in Applied Mathematics, Proceedings of the Summer Seminar, Boulder, CO*, 1957.
- [25] D. Braess. *Finite Elements: Theory, Fast Solvers, and Applications in Solid Mechanics*. Cambridge University Press, 2007.
- [26] L. Chen. iFEM: an innovative finite element methods package in MATLAB. *In Preparation*, 2008.
- [27] P. Ciarlet and P.-A. Raviart. The combined effect of curved boundaries and numerical integration in isoparametric finite element methods. *Math. Foundation of the FEM with Applications to PDE*, pages 409–474, 1972.
- [28] D. Cioranescu and P. Donato. *An Introduction to Homogenization (Oxford Lecture Series in*

- Mathematics and Its Applications*, 17). Oxford University Press, USA, 2000.
- [29] R. Cools. Constructing cubature formulae: the science behind the art. *Acta Numerica*, 6:1–54, 1997.
 - [30] E. De Giorgi and S. Spagnolo. Sulla convergenza degli integrali dell’energia per operatori ellittici del secondo ordine. *Boll. Un. Mat. Ital.*, 8(4):391–411, 1973.
 - [31] W. E and B. Engquist. The heterogeneous multiscale methods. *Commun. Math. Sci.*, 1:87–132, 2003.
 - [32] W. E, B. Engquist, and Z. Huang. Heterogeneous multiscale method: a general methodology for multiscale modeling. *Physical Review B*, 67(9):092101, 2003.
 - [33] W. E, B. Engquist, X. Li, W. Ren, and E. Vanden-Eijnden. The Heterogeneous Multiscale Method: A Review. *Commun Comput Phys*, 2:367–450, 2007.
 - [34] W. E, P. Ming, and P. Zhang. Analysis of the heterogeneous multiscale method for elliptic homogenization problems. *American Mathematical Society*, 18(1):121–156, 2005.
 - [35] Y. Efendiev and T. Y. Hou. *Multiscale Finite Element Methods: Theory and Applications*. Springer, Berlin, 2009.
 - [36] A. Ern and J.L. Guermond. *Theory and practice of finite elements*. Springer Verlag, 2004.
 - [37] M.B. Giles and E. Suli. Adjoint methods for PDEs: a posteriori error analysis and postprocessing by duality. *Acta Numerica*, 11:145–236, 2002.
 - [38] T. Grätsch and K.J. Bathe. A posteriori error estimation techniques in practical finite element analysis. *Computers & Structures*, 83(4-5):235–265, 2005.
 - [39] P. Henning and M. Ohlberger. A-posteriori error estimation for a heterogeneous multiscale method for monotone operators and beyond a periodic setting. Preprint 01/11 - N, FB 10, Universität Münster, 2011.
 - [40] V.H. Hoang and Ch. Schwab. High-dimensional finite elements for elliptic problems with multiple scales. *Multiscale Modeling & Simulation*, 3:168–194, 2005.
 - [41] T.Y. Hou, X.H. Wu, and Z. Cai. Convergence of a Multiscale Finite Element Method for Elliptic Problems with Rapidly Oscillating Coefficients. *Mathematics of Computation*, 68(227):913–943, 1999.
 - [42] T.J.R. Hughes. Multiscale phenomena: Green’s functions, the Dirichlet-to-Neumann formulation, subgrid scale models, bubbles and the origins of stabilized methods* 1. *Computer methods in applied mechanics and engineering*, 127(1-4):387–401, 1995.
 - [43] T.J.R. Hughes, G.R. Feijoo, L. Mazzei, and J.B. Quinicy. The variational multiscale method—a paradigm for computational mechanics. *Computer methods in applied mechanics and engineering*, 166(1-2):3–24, 1998.
 - [44] V. V. Jikov, S. M. Kozlov, and O. A. Oleinik. *Homogenization of Differential Operators and Integral Functionals*. Springer-Verlag Telos, 1994.
 - [45] O.A. Ladyzhenskaya. *Boundary value problems of mathematical physics*. Springer-Verlag New York, 1985.
 - [46] M.G. Larson and A. Målqvist. Adaptive variational multiscale methods based on a posteriori error estimation: Duality techniques for elliptic problems. *Multiscale Methods in Science and Engineering*, pages 181–193, 2005.
 - [47] M.G. Larson and A. Målqvist. Adaptive variational multiscale methods based on a posteriori error estimation: Energy norm estimates for elliptic problems. *Computer Methods in Applied Mechanics and Engineering*, 196(21-24):2313–2324, 2007.
 - [48] A.M. Matache, I. Babuška, and Ch. Schwab. Generalized p-FEM in homogenization. *Numerische Mathematik*, 86(2):319–375, 2000.
 - [49] P. Morin, R.H. Nochetto, and K.G. Siebert. Convergence of adaptive finite element methods. *SIAM review*, 44(4):631–658, 2002.
 - [50] François Murat and Luc Tartar. H-convergence, topics in the mathematical modeling of composite materials. *Progr. Nonlinear Differential Equations Appl.*, 31:21–43, 1997.
 - [51] G. Nguetseng. A general convergence result for a functional related to the theory of homogenization. *SIAM Journal on Mathematical Analysis*, 20:608, 1989.
 - [52] R.H. Nochetto, A. Veiser, and M. Verani. A safeguarded dual weighted residual method. *IMA journal of Numerical Analysis*, 29(1):126–140, 2009.
 - [53] A. Nonnenmacher. *Adaptive Finite Element Methods for Multiscale Partial Differential Equations*. PhD thesis, EPFL, 2011.
 - [54] J.T. Oden and S. Prudhomme. Goal-oriented error estimation and adaptivity for the finite element method. *Computers & Mathematics with Applications*, 41(5-6):735 – 756, 2001.
 - [55] J.T. Oden, S. Prudhomme, A. Romkes, and P.T. Bauman. Multiscale modeling of physical phenomena: Adaptive control of models. *SIAM Journal on Scientific Computing*, 28(6):2359–2392, 2006.
 - [56] M. Ohlberger. A posteriori error estimates for the heterogeneous multiscale finite element

- method for elliptic homogenization problems. *SIAM Multiscale Modeling & Simulation*, 4:88–114, 2005.
- [57] S. Prudhomme and J.T. Oden. On goal-oriented error estimation for elliptic problems: application to the control of pointwise errors. *Computer Methods in Applied Mechanics and Engineering*, 176(1-4):313–331, 1999.
- [58] P.A. Raviart. The use of numerical integration in finite element methods for solving parabolic equations. *Miller, J. J. H. (ed.), Topics in Numerical Analysis, Academic Press*, pages 233–264, 1973.
- [59] H.J. Schmid. On cubature formulae with a minimal number of knots. *Numerische Mathematik*, 31(3):281–297, 1978.
- [60] A. Schmidt and K. Siebert. *Design of Adaptive Finite Element Software: the Finite Element Toolbox Alberta*. Springer, Berlin, 2005.
- [61] E. Suli. Review of the book *Adaptive finite element methods for differential equations* by W. Bangerth and R. Rannacher. *Math. Comp.*, 74:1033–1052, 2004.
- [62] R. Verfürth. *A Review of A Posteriori Error Estimation & Adaptive Mesh-Refinement Techniques*. Wiley-Teubner, 1996.
- [63] O. Zienkiewicz. *The Finite Element Method*. Elsevier/Butterworth-Heinemann, Amsterdam, 2005.

Recent publications :

MATHEMATICS INSTITUTE OF COMPUTATIONAL SCIENCE AND ENGINEERING
Section of Mathematics
Ecole Polytechnique Fédérale
CH-1015 Lausanne

- 01.2011** T. LASSILA, A. QUARTERONI, G. ROZZA:
A reduced basis model with parametric coupling for fluid-structure interaction problems
- 02.2011** A. QUARTERONI, G. ROZZA, A. MANZONI:
Certified Reduced Basis Approximation for Parametrized Partial Differential Equations and Applications
- 03.2011** M. LOMBARDI, N. PAROLINI, A. QUARTERONI, G. ROZZA:
Numerical simulation of sailing boats: dynamics, FSI and shape optimization
- 04.2011** P. BLANCO, P. GERVASIO, A. QUARTERONI:
Extended variational formulation for heterogeneous partial differential equations
- 05.2011** A. MANZONI, A. QUARTERONI, G. ROZZA:
Model reduction techniques for fast blood flow simulation in parametrized geometries
- 06.2011** M. ASTORINO, J. BECERRA SAGREDO, A. QUARTERONI:
A modular lattice Boltzmann solver for GPU computing processors
- 07.2011** L. IAPICHINO, A. QUARTERONI, G. ROZZA:
A reduced basis hybrid method for the coupling of parametrized domains represented by fluidic networks
- 08.2011** T. LASSILA, A. MANZONI, G. ROZZA:
On the approximation of stability factors for general parametrized partial differential equations with a two-level affine decomposition
- 09.2011** M. DISCACCIATI, A. QUARTERONI, S. QUINODOZ:
Numerical approximation of internal discontinuity interface problems
- 10.2011** A. C. I. MALOSSI, P. J. BLANCO, S. DEPARIS:
A two-level time step technique for the partitioned solution of one-dimensional arterial networks
- 11.2011** PH. BLANC
On a problem in relation with the values of the argument of the Riemann zeta function in the neighborhood of points where zeta is large
- 12.2011** T. LASSILA, A. MANZONI, A. QUARTERONI, G. ROZZA:
A reduced computational and geometrical framework for inverse problems in haemodynamics
- 13.2011** D. KRESSNER, C. TOBLER:
Low-rank tensor Krylov subspace methods for parametrized linear systems
- 01.2012** A. ABDULLE, A. NONNENMACHER:
A posteriori error estimate in quantities of interest for the finite element heterogeneous multiscale method